Brain and Cognition 141 (2020) 105565

Contents lists available at ScienceDirect

Brain and Cognition

journal homepage: www.elsevier.com/locate/b&c

Prompting future events: Effects of temporal cueing and time on task on brain preparation to action

Marika Berchicci[a,*], Valentina Sulpizio[b,c], Giovanni Mento[d], Giuliana Lucci[e], Nicole Civale[c,f], Gaspare Galati[c,f], Sabrina Pitzalis[a,c], Donatella Spinelli[a,c], Francesco Di Russo[a,c]

[a] Department of Movement, Human and Health Sciences, University of Rome "Foro Italico", Rome 00135, Italy
[b] Department of Biomedical and Neuromotor Sciences, University of Bologna, Bologna, Italy
[c] IRCCS Santa Lucia Foundation, Rome 00179, Italy
[d] Department of General Psychology, University of Padua, Padua 35131, Italy
[e] Department of Human Sciences, Marconi University, Rome, Italy
[f] Department of Psychology, University of Rome "La Sapienza", Rome 00185, Italy

ARTICLE INFO

Keywords:
EEG
fMRI
Timing
Prefrontal cortex
Proactive control
Go/No-go

ABSTRACT

Prediction about event timing plays a leading role in organizing and optimizing behavior. We recorded anticipatory brain activities and evaluated whether temporal orienting processes are reflected by the novel prefrontal negative (pN) component, as already shown for the contingent negative variation (CNV). Fourteen young healthy participants underwent EEG and fMRI recordings in separate sessions; they were asked to perform a Go/No-Go task in which temporal orienting was manipulated: the *external* condition (a visual display indicating the time of stimulus onset) and the *internal* condition (time information not provided). In both conditions, the source of the pN was localized in the pars opercularis of the iFg; the source of the CNV was localized in the supplementary motor area and cingulate motor area, as expected. Anticipatory activity was also found in the occipital-parietal cortex. Time on task EEG analysis showed a marked learning effect in the internal condition, while the effect was minor in the external condition. In fMRI, the two conditions had a similar pattern; similarities and differences of results obtained with the two techniques are discussed. Overall, data are consistent with the view that the pN reflects a proactive cognitive control, including temporal orienting.

1. Introduction

Preparation can be defined as the process by which an organism is getting ready to cope with future events; thus, preparation is a fundamental brain function that facilitates sensory, cognitive and motor processing. Brain correlates of action preparation have been largely investigated in event-related potential (ERP) studies, showing slow-rising negative waves (for a review, see Di Russo et al., 2017), such as the Bereitschaftspotential (BP) or readiness potential (RP) (e.g. Kornhuber & Deecke, 1965; Vaughan, Costa, & Ritter, 1968) and the contingent negative variation (CNV) (Walter, Cooper, Aldridge, McCallum, & Winter, 1964). The BP is especially evident before any voluntary movement in tasks not involving a cue; it is prominent over medial central derivations, and its source has been localized in the cingulate motor area (CMA) and the supplementary motor area (SMA) for both self-paced (e.g. Shibasaki & Hallett, 2006) and externally triggered (Cunnington, Iansek, Bradshaw, & Phillips, 1995; Di Russo et al., 2005, 2016; Jahanshahi et al., 1995; Jenkins, Jahanshahi, Jueptner, Passingham, & Brooks, 2000; Sulpizio et al., 2017) movements. The CNV occurs when a warning stimulus (S1) cues an upcoming imperative stimulus (S2) requiring a motor response, and its source has been localized in the SMA and/or the medial premotor cortex (Mento & Valenza, 2016; Mento et al., 2013, 2015; Pfeuty, Ragot, & Pouthas, 2005). The BP, representing the electrophysiological index of motor readiness, and the late CNV share the same sources (Brunia, van Boxtel, & Böcker, 2011) and function (see Brunia, 1988; for a review, see van Boxtel & Böcker, 2004), whereas the overall CNV represents the sum of activities related to different processes, such as cue perception and categorization, expectancy processes related to the information provided by the cue, motor preparation processes (for a review, see van Boxtel & Böcker, 2004), and temporal anticipation of events (Los & Heslenfeld, 2005; Macar, Vidal, & Casini, 1999; Mento et al., 2013, 2015; Mento & Vallesi, 2016; Monfort, Pouthas, & Ragot, 2000; Pfeuty, Ragot, & Pouthas, 2003; Trillenberg, Verleger, Wascher,

* Corresponding author at: Department of Movement, Human and Health Sciences, University of Rome "Foro Italico", Piazza Lauro de Bosis 15, Rome 00135, Italy.
E-mail address: marika.berchicci@uniroma4.it (M. Berchicci).

https://doi.org/10.1016/j.bandc.2020.105565
Received 27 December 2019; Received in revised form 11 March 2020; Accepted 19 March 2020
Available online 13 April 2020

Wauschkuhn, & Wessel, 2000; see Mento, 2013 for a review). In particular, temporal orienting during the preparation phase may increase participant's readiness to respond around the time of the expected event with shorter response times, as suggested by CNV studies (Macar & Vidal, 2003; Mento et al., 2013, 2015; Pfeuty et al., 2005).

More recently, another slow-rising negative wave has been described. This component is likely part of the Stimulus Preceding Negativity (SPN) "family", although the pN was observed in tasks different from those eliciting SPN and its sources were localized on different brain regions (Brunia & Damen, 1988; Brunia et al., 2011; Gómez, Flores, & Ledesma, 2007; Gómez, Marco, & Grau, 2003; van Boxtel & Böcker, 2004). We first observed the pN in visual-motor discriminative tasks (the Go/No-go) in the absence of a cue and with variable inter-stimulus interval (ISI) (Berchicci, Lucci, Pesce, Spinelli, & Di Russo, 2012). This preparatory ERP component was named prefrontal negativity (pN), because it was prominent over prefrontal scalp regions (Berchicci et al., 2013, 2014, 2015, 2016; Di Russo et al., 2016, 2017; Gonçalves et al., 2018; Lucci, Berchicci, Perri, Spinelli, & Di Russo, 2016; Perri et al., 2014a, 2015; Ragazzoni et al., 2019; Sulpizio et al., 2017); in particular, studies associating fMRI and ERP techniques localized its source in the pars opercularis of the inferior frontal gyrus (iFg) (Di Russo et al., 2016; Ragazzoni et al., 2019; Sulpizio et al., 2017). The iFg (Broadmann area 44) is implicated in response inhibition tasks (e.g. Aron, 2011), such as the Stop-signal and the Go/No-go (Hampshire, Chamberlain, Monti, Duncan, & Owen, 2010). Since this latter task not only requires inhibition, but involves a wide range of cognitive functions, especially executive functions (see Criaud & Boulinguez, 2013 for a review), it has been proposed that the pN represents an electrophysiological index of the top-down proactive cognitive control needed to accomplish the task (Berchicci et al., 2012, 2013, 2015, 2016; Berchicci, Lucci, Perri, Spinelli, & Di Russo, 2014; Di Russo et al., 2016, 2019; Gonçalves et al., 2018; Perri et al., 2014a, 2014b, 2015, 2016). The proactive control is a form of anticipation and regulation of the behavior engaged before either external or internal events (Braver, Paxton, Locke, & Barch, 2009), which includes proactive inhibitory control (Bianco, Berchicci, Perri, Spinelli, & Di Russo, 2017; Frank, 2006; Gillies & Willshaw, 1998). The pN component is modulated by several cognitive factors, such as spatial attention (Berchicci et al., 2019), task complexity (Berchicci, Lucci, & Di Russo, 2013; Berchicci, Lucci, Perri, Spinelli, & Di Russo, 2014), individual response consistency (Perri, Berchicci, Lucci, Spinelli, & Di Russo, 2015), and age-related cognitive decline (Berchicci et al., 2012); the pN was also associated with proactive inhibition of an upcoming response, when right-lateralized (Bianco et al., 2017; Lucci et al., 2016), and top-down cognitive control, when the activation was bilateral (Berchicci et al., 2012, 2013, 2015, 2016; Berchicci et al., 2014; Di Russo et al., 2016; Perri et al., 2014a, 2015, 2016).

The main purpose of the present study was to evaluate whether the pN might reflect also processing related to temporal orienting. In a previous study manipulating the temporal orienting function with external cues and constant foreperiods (Berchicci, Lucci, Spinelli, & Di Russo, 2015), we failed to record the standard pN component (the component had positive polarity). Thus, the question is still open on whether the proactive cognitive control reflected by the pN component would also include temporal orienting. Further, to better define the sources of prefrontal (pN) and central (CNV) scalp-recorded activities, individual ERP recordings were associated to fMRI recordings from the same participant.

Available fMRI data show that the frontal network is activated during action preparation (Brass & von Cramon, 2002; for a review see Hoffmann et al., 2018). Within this network, the main regions activated during task-related processing are the premotor cortex, involved in movement preparation, and the dorsolateral and inferior frontal cortex, associated with the stimulus–response association (MacDonald, Cohen, Stenger, & Carter, 2000; Nagahama et al., 2001). Further, it has been widely accepted that the frontoparietal network plays a key role in the anticipatory preparation of a response, with the dorsolateral prefrontal cortex and the posterior parietal cortex involved in top-down control of action, action inhibition and preparation to inhibit (Aron & Poldrack, 2006; Chikazoe et al., 2009; Jamadar, Hughes, Fulham, Michie, & Karayanidis, 2010).

In the present experiment, the temporal orienting was induced/not induced by the presence/absence of external information about the temporal onset of the imperative stimulus. In a Go/No-go experiment, a neutral cue (as it regards the foreperiod duration) was used, the ISI was variable, the foreperiod was constant, and the temporal predictability was manipulated, leading to two conditions. In the first condition (called *external*), the foreperiod was filled with a visual display, i.e. a circle moving toward the center, which exactly indicated the time of stimulus onset (as in Berchicci et al., 2015); thus, participants could synchronize their action to stimulus onset by exploiting this external visual information. In the second condition (called *internal*), no external information was given during the foreperiod.

If the pN reflects temporal orienting, we may expect to record different prefrontal activities in the external and internal conditions, because temporal orienting should be more robust in the former than the latter case. Alternatively, if similar prefrontal activities were recorded in the two conditions, one may derive that the pN component did not reflect any processing related to temporal orienting or that temporal orienting was similarly active in both conditions. The CNV was also compared between conditions to confirm results of previous CNV studies. Since information about temporal predictability may be present in distributed patterns of fMRI activation across voxels, thus making difficult to detect potential differences between conditions when looking at each voxel independently as in the mass-univariate method (see Norman, Polyn, Detre, & Haxby, 2006 for a review), we employed a multivariate pattern analysis (MVPA) on fMRI data to determine whether external and internal conditions elicited distinct patterns of activations.

Considering the possibility of implicit learning throughout the experiment, we were interested in comparing the time on task effects in the two conditions for the pN component, as well as the CNV component. Implicit learning could reduce the amount of resources needed for performance during the preparation stage (Mento & Valenza, 2016); however, the amount of learning may be different in the two conditions. The characteristics of the external condition should immediately induce temporal orienting; thus, little space would remain for learning in this case. Learning should be more relevant in the internal condition: in the initial trials the subject does not perceive/register the informational value of the warning stimulus (and instructions did not illustrate its value); after a certain number of trials, it becomes an effective signal to predict the stimulus onset time, likely based on both intentional and unintentional orienting mechanisms (Los & Heslenfeld, 2005). Thus, only in the last trials of the internal condition we may fully observe the effect of temporal orienting. Comparison of time on task effect in the two conditions may support interpretations in terms of temporal orienting.

Previous studies have shown that information about timing of future events improves motor performance (e.g. Coull, Cheng, & Meck, 2011; Nobre, Correa, & Coull, 2007; Mento, Tarantino, Vallesi, & Bisiacchi, 2015; Mento & Vallesi, 2016), reducing response times (for reviews see: Coull & Nobre, 1998; Requin, 1969; Posner, Snyder, & Davidson, 1980; Correa, Triviño, Pérez-Dueñas, Acosta, & Lupiáñez, 2010). Thus, we expect that the present external condition would produce shorter response times than the internal condition, and this advantage could be more evident before than after learning. Overall, we tested the time on task effect at both behavioral and electrophysiological levels, comparing first and last trials in both conditions.

2. Experimental procedures

2.1. Participants

Fourteen participants volunteered for the ERP experiment (6 females, mean age ± SD: 21.6 ± 2.4 years) and for the structural MRI and fMRI scanning. All participants were healthy, with no history of neurological, psychiatric, or somatic problems. The participants did not take medication during the experimental sessions and had normal or corrected-to-normal vision. All participants were right-handed as assessed by the Edinburgh Handedness Inventory (Oldfield, 1971). All procedures were reviewed and approved by the Santa Lucia Foundation Ethical Committee. All participants gave their informed consent according to the Declaration of Helsinki.

2.2. Stimuli and task

For the electroencephalographic (EEG) recording, the participants were seated in a darkened room with a keyboard under his/her right hand; the response was given by the right index finger. During the fMRI recording, participants laid in the scanner on their back; their right hand was positioned palm down on a button board and response was given by pushing this device with the hand, while during the structural MRI, participants laid in the scanner on their back and had no task to perform.

Participants performed the Go/No-go task described below in two separate sessions, i.e., *external* and *internal* conditions (for EEG in separate days, while for fMRI in separate runs within the same day; the difference is due to the number of trials). The order of external and internal conditions was counterbalanced across participants.

The Go/No-go consisted in the presentation of a squared visual configuration (imperative stimulus or stimulus) presented centrally (subtending 4° × 4°) on a dark gray background (Fig. 1) using Presentation™ software. The total number of stimuli was four, which were randomly displayed for 250 ms with equal probability (p = 0.25) and were counterbalanced across participants. Stimuli were made up by vertical bars, horizontal bars, and vertical plus horizontal bars differently arranged (see the inset of Fig. 1). Two configurations were defined as targets (Go stimuli), and two were defined as non-targets (No-go stimuli). Participants were asked to respond as fast and accurately as possible to Go stimuli (p = 0.50) by pressing a button with their right index finger and withhold the response when No-go stimuli (p = 0.50) appeared.

Each trial started with a fixation point consisting of a white cross (0.15° × 0.15° of visual angle) in the center of the computer monitor with a variable duration between 2750 and 4250 ms. This long interval minimizes the possible effect of trial n − 1 on trial n. After this variable interval, the color of the fixation cross changed to green (cue), then the two conditions (external and internal) had different features. Go and No-go trials were interleaved with "relax" and "null" trials. Relax trials consisted in a red cross (replacing the green cross) with a 2500 ms duration; in these trials, no stimulus was presented and, then, no response was required. These trials were included in both ERP and fMRI as a control condition for evaluating the cue-related orienting and perceptual brain activities and were used for the fMRI data analysis. The subject was instructed in advance that the red cross was not followed by any stimulus. Additionally, in the fMRI paradigm only, null trials were inserted. In these trials, no stimulus was displayed, and the white fixation cross was steady on the screen for the entire trial duration. The trial duration varied from 5000 to 6500 ms (5750 ± SD 536 ms).

The two conditions differed after the presentation of the green cross. In the external condition, the green cross was present alone for 250 ms, and in the following 2000 ms a sequence of 16 green concentric circles (duration 125 ms each) with progressively smaller diameters (from 3.75° to 0.15°) was displayed on the screen (always in presence of the green fixation cross); this sequence was perceived as a circle moving toward the fixation cross. The imperative stimulus was displayed immediately after the offset of the smallest circle. In the internal condition, after the cue (color change from white to green) no other stimuli were displayed; thus, the green fixation cross was displayed for 2250 ms, then the imperative stimulus appeared (Fig. 1).

In the ERP experiment, 10 runs were executed (400 Go and 400 No-go trials) for each experimental condition. The whole experiment lasted

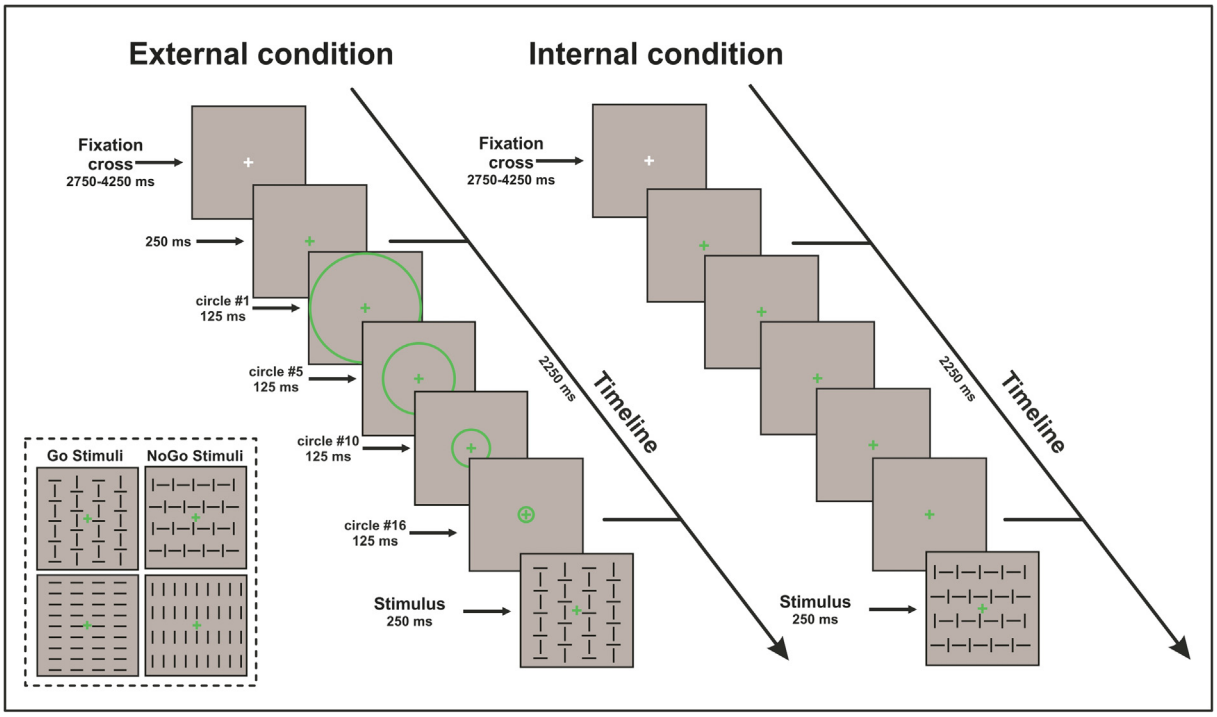

Fig. 1. Representation of the Go/No-go trials in the external and internal conditions. The inset shows the four possible configurations (stimuli).

approximately 2 h per condition; the participants come twice to the lab to perform the two conditions in a counterbalanced order.

In the fMRI experiment, each subject completed eight functional acquisition scans (four external and four internal conditions) of Go/No-go task, each including 18 target trials and 18 non-target trials, plus 18 relax and 8 null trials. Each scan lasted 6′20″, and, the order of trials' presentation was randomized within each scan. The order of the scans was counterbalanced across participants.

The participants were initially familiarized with the task and a detailed explanation of conditions was provided, especially about the informative role of the warning signal. In addition, one warming up run for each condition always preceded the experiment. The experiments were separated by an inter-session time of approximately two weeks, and the session order was counterbalanced across participants.

2.3. Behavioral data analysis

Response accuracy was measured by the percentage of omission (OM%: missed responses or responses longer than 1000 ms) and commission (CE%: responses to No-go stimuli) errors. The median response time (RTs) for correct trials was calculated for each participant; whereas, the mean value of the RTs was considered at the group level. The mean RT and its standard deviation (SD) were used to calculate the intra-individual coefficient of variation (ICV = SD/mean RT). Paired-samples t-tests were separately performed for each behavioral measure between conditions (external vs. internal), separately for ERP and fMRI experiments. Further, a 2 (Experiment: ERP vs. fMRI) X 2 (Condition: external vs. internal) analysis of variance (ANOVA) was performed for mean RTs, OM%, CE% and ICV to compare the behavioral performances between the two techniques.

To calculate the time on task effect, the mean RTs of the first quartile of trials (ERP: N = 100; fMRI: N = 18) and the last quartile of trials (ERP: N = 100; fMRI: N = 18) for both conditions were separately (ERP and fMRI) submitted to a 2 (first vs. last trials) × 2 (external vs. internal) ANOVA. The alpha level was fixed at 0.05 for all analyses.

2.4. ERP experiment

2.4.1. Recording and analysis

Visual stimuli were presented through a computer display placed at 114 cm distance. EEG was recorded using two BrainAmp amplifiers connected to 64-active sensors ActiCap. Data were collected using the BrainVision Recorder 1.2 and analyzed using Analyzer 2.1 software (BrainProducts GmbH., Munich, Germany). Electrodes were mounted according to the 10–10 International System, initially referenced to the left mastoid (M1) and, then, off-line re-referenced to the M1-M2 average. EEG was digitized at 250 Hz, amplified (bandpass of 0.01–80 Hz) and stored for off-line analysis. Horizontal eye movements (electrooculogram, EOG) were monitored with electrodes placed at the left and right outer canthi. Blinks were recorded with electrodes placed below and above the left eye. Eye movements were identified and eliminated using the independent component analysis (ICA; Jung et al., 2000) algorithm. Remaining artifacts and signals exceeding ± 50 μV were discarded using a semi-automatic computerized artifact rejection approach. Trials with RTs outside 150–1000 ms time window, omissions and commission errors were discarded from further analysis. After artifact rejection, the signal was segmented and averaged. Finally, to reduce high-frequency noise, the time-locked EEG grand-averages were high-pass filtered using an IIR filter (30 Hz; 48 dB/oct). On average 4% of trials were rejected.

To evaluate pre-stimulus activity, both external and internal conditions were segmented collapsing together Go and No-go trials into 3500 ms epochs, starting 2500 ms before and ending 1000 ms after the stimulus onset, with the first 200 ms (−2500/−2300 ms) as baseline. A mass-univariate analysis was performed on the data (as described in the Section 2.4.2), allowing a data-driven analysis, which reduces the experimenter bias and provides a point-by-point resolution plotted on the whole cortex. To investigate the time on task effect, the ERPs were also separately averaged into the first and last quartile of trials, referred to as first and last trials, and were submitted to the same mass-univariate analysis.

2.4.2. Statistical analyses

We used a data-driven approach to analyse the pre-stimulus phase, in order to avoid any bias about results. The statistical analyses of pre-stimulus data were performed by using the Mass Univariate Analysis toolbox (Groppe, Urbach, & Kutas, 2011), because it provides good spatial and temporal resolutions, while maintaining reasonable limits on the likelihood of false discoveries. A cluster-based permutation test based on the cluster mass statistic using the original data and 2000 random within-participant permutations of the data was used. This non-parametric statistical approach allowed us to test the presence of statistically significant amplitude differences in pre-stimulus ERPs between the external and internal conditions, and to directly estimate these statistical amplitude differences on the scalp electrodes. Electrodes within approximately 1.5 cm of one another were considered spatial neighbours and adjacent time points were considered temporal neighbours. All pairs (internal vs. external) whose t-values were larger than the pre-determined threshold of ± 2.14 (corresponding to a Family Wise Error corrected alpha value of 0.05) were considered significant.

Further, statistical parametric maps of t values reflecting the differences between conditions were generated. To visualize the ERP voltage topography, spherical spline interpolated top-flat views 120° wide were constructed (BrainVision Analyzer 2.1).

2.4.3. ERP-fMRI combination

Estimation of the time-course of dipolar sources of the pre-stimulus ERP components were performed using Brain Electrical Source Analysis (BESA 2000 v.5.1.8; Megis Software GmbH, Gräfelfing, Germany). We used a realistic approximation of the head, with the radius obtained from the average of the group of subjects (81 mm) determined using a Polhemus Fastrack digitizer. The BESA algorithm calculates the scalp distribution obtained for a given dipole model (forward solution) and compares it to the actual ERP distribution to estimate the location and the orientation of multiple equivalent dipolar sources. To allow the measurement of the time-course of each brain area, the grand-average ERP data were seeded on the fMRI activations using an fMRI-informed EEG analysis (see Bledowski et al., 2006; Carlson, Foti, Mujica-Parodi, Harmon-Jones, & Hajcak, 2011; Crottaz-Herbette & Menon, 2006); following this approach, the fMRI information was used to solve the inverse problem of the ERP source localization. The regions of interest (ROI) were selected by clustering the fMRI activations (see Section 2.5.3). Specifically, for each regional peak, we grouped together all neighboring voxels at a maximum distance of 8 mm from the peak and the resulting coordinates (Table 1) were used to seed the sources. To avoid the estimation of interacting dipoles, we selected solutions with relatively low dipole moments setting an "energy" constraint (weighted 20% in the compound cost function as opposed to 80% for the residual variance [RV]). The best set of parameters was identified by searching for a minimum in the compound cost function in an iterative manner. The selection of both interval and orientation of the dipoles was based on the timing and the scalp topography of the ERPs, minimizing the cross-talk and interactions between the sources. Modeling followed a sequential approach according to which the dipoles that accounted for the earlier portions of the ERP waveform were maintained in place as additional dipoles were added.

Table 1
Talairach coordinates of local maxima found in the omnibus F-contrast. LH: Left Hemisphere; RH: Right Hemisphere.

Local maxima		Coordinates		
		x	y	z
M1/S1	LH	−36	−25	53
aIPs	LH	−50	−29	43
SMA/CMA	LH	−2	−4	47
	RH	7	8	50
iFg	LH	−26	23	3
	RH	28	23	1
aIns	LH	−37	−5	14
	RH	40	−6	10
hIPs	LH	−36	−49	48
	RH	31	−60	42
pIPs	LH	−27	−67	42
	RH	31	−60	42
Striate + Extrastriate	LH	−27	−88	5
	RH	31	−88	8

2.5. fMRI experiment

2.5.1. Apparatus and procedures

Images were acquired using a 3T Siemens Allegra MR system (Siemens Medical systems, Erlangen, Germany) operating at the Neuroimaging Laboratory of Santa Lucia Foundation, using a standard receiving/transmitting head coil. Stimuli were generated by a control computer located outside the MR room, running in-house software (Galati et al., 2008) implemented in MATLAB (The MathWorks Inc., Natick, MA, USA). An LCD video projector with customized lens was used to project visual stimuli to a back-projection screen mounted inside the MR tube and visible through a mirror mounted inside the head coil. Presentation timing was controlled and triggered by the acquisition of fMRI images. Responses were given through push buttons connected to the control computer via optic fibers.

Echo-planar functional MR images (TR = 2 s, TE = 30 ms, flip angle = 70 deg, 64 × 64 image matrix, 3 × 3 mm in-plane resolution, 30 slices, 4.5 mm slice thickness with no gap, interleaved excitation order) were acquired in the AC–PC plane using blood-oxygenation level-dependent imaging (Kwong et al., 1992). From the superior convexity, sampling included all the cerebral cortex, excluding only the ventral portion of the cerebellum. A three-dimensional high-resolution anatomical image was also acquired for each subject (Siemens MPRAGE sequence, TR = 2 s, TE = 4.38 ms, flip angle = 8 deg, 512 × 512 image matrix, 0.5 × 0.5 mm in-plane resolution, 176 contiguous 1 mm thick sagittal slices). The first four volumes of each scan were discarded to achieve steady-state, and the experimental task started at the beginning of the fifth image.

2.5.2. Image preprocessing

Images were preprocessed and analyzed using SPM12 (Wellcome Department of Cognitive Neurology, London, UK). Functional time series from each subject were first temporally corrected for slice timing, using the middle slice acquired in time as a reference, and then spatially corrected for head movements, using a least-squares approach and six parameter rigid body spatial transformations. They were then spatially normalized using an automatic nonlinear stereotaxic normalization procedure (final voxel size: 3 × 3 × 3 mm) and spatially smoothed with a three-dimensional Gaussian filter (6 mm full-width-half-maximum). Data for multivariate analyses (see below) were left unsmoothed. The template image for spatial normalization was based on average data provided by the Montreal Neurological Institute (Mazziotta, Toga, Evans, Fox, & Lancaster, 1995) and conformed to a standard coordinate referencing system (Talairach & Tournoux, 1988).

2.5.3. Univariate analysis

Images were analyzed using a standard random-effects procedure. The time series of functional MR images obtained from each participant were analyzed separately. The effects of the experimental paradigm were estimated on a voxel-by-voxel basis, according to the general linear model extended to allow the analysis of fMRI data as a time series. The model was high-pass filtered to remove low-frequency confounds with a period above 128 s. Serial correlation in the fMRI time series were estimated with a restricted maximum likelihood (ReML) algorithm using an autoregressive AR(1) model during parameter estimation, assuming the same correlation structure for each voxel, within each scan. The ReML estimates were then used to whiten the data.

To capture sustained pre-stimulus activity showed by ERP data, we modeled evoked fMRI responses as box-car functions spanning the time interval from the beginning of a trial to the stimulus presentation (2250 ms), representing an ideally constant and sustained neural activity level for the whole-time interval. Box-car functions were then convolved with a canonical hemodynamic response function, chosen to represent the relationship between neuronal activation and blood flow changes (Boynton, Engel, Glover, & Heeger, 1996; Friston, Fletcher, Josephs, Holmes, & Rugg, 1998). Separate regressors were included for each trial type (Go/external, Go/internal, No-go/external, No-go/internal), yielding parameter estimates for the average hemodynamic response evoked by each one. For both external and internal conditions, go trials with response omissions and No-go trials with false alarms were modeled by separate regressors and then excluded from further analyses.

The two experimental conditions (external vs. internal) were studied in separate scans, but the comparison between the two was possible by using an independent and common control condition (Relax trials) and a low-level baseline (Null trials) in all scans. Thus, we looked at brain regions more implicated in at least one experimental condition as compared to the control condition (Relax trials). The resulting map of the F statistic was thresholded at $p < 0.01$, corrected for multiple comparisons based on family-wise error (FWE), with a cluster size > 20 voxels. For each subject and region, we computed a regional estimate of the amplitude of the hemodynamic response in each experimental task by entering a spatial average (across all voxels in the region) of the pre-processed time series into the individual general linear models. Thus, the regional hemodynamic response was analyzed by means of a 2 × 2 ANOVA with task (Go and No-go) and condition (external and internal) as factors. Post-hoc comparisons were conducted using Bonferroni correction.

To further explore any task-dependent activity as a function of learning, we analyzed the BOLD signal change of the above-mentioned regions (see Fig. 6) as a function of condition (external and internal) and time-on-task. For each run, stimuli were grouped in quartiles as a function of presentation time, and the analysis was conducted including the first and fourth quartile (called first and last trials) of both Go and No-go trials.

2.5.4. Multivariate classification analysis

An alternative strategy to show the neural substrates of temporal informative cue effects was based on a multivariate classification analysis, where a classifier was trained to discriminate multi-voxel patterns of estimated BOLD responses to pairs of external and internal trials (see Norman et al., 2006 for a review). As a preliminary step for multivariate pattern analysis, we used a general linear model in which trials related to each of the two conditions (external and internal) were modeled by separate regressors, to estimate the magnitude of the response at each voxel for each trial. Multivariate analyses were thus conducted on patterns extracted from the regions activated by the univariate analysis (see above). We trained a linear discriminant analysis (LDA) classifier to learn the association between the category (external or internal) and the corresponding multivoxel pattern. This was achieved by splitting the data set into a training set and a test set. We used an odd–even

cross-validation procedure to test classification outcomes on a data set independent from that used for training the classifier: data from odd runs were used to train the classifier and data from even runs were used to evaluate prediction accuracy. The resulting classification outcomes were averaged across cross-validation folds. For each classification analysis, we compared the between-subject distribution of classification accuracies with chance level (i.e., 0.5) by means of one-sample t-tests, applying Bonferroni's correction for multiple comparisons, as performed in previous studies (Boccia et al., 2014, 2016; Sulpizio, Committeri, & Galati, 2014). Classification outcomes significantly above chance were taken as evidence of discrimination between external and internal conditions.

3. Results

3.1. Behavioral results

In the ERP experiments, no significant differences between conditions were found for accuracy ($p > 0.2$, CE%: 7.0 and 6.4 in internal and external, respectively; Om%: 1.5 and 1.2 in internal and external, respectively) and ICV ($p > 0.1$, ICV: 0.17 ± 0.02 and 0.17 ± 0.024 in internal and external, respectively). As for RTs, a two-tailed *t*-test showed that participants were faster ($t_{13} = -4$, $p = 0.001$) in the external (429 ± 50 ms) than internal (499 ± 48 ms) condition. Further, we found a main time on task effect ($F_{1,13} = 5.83$, $p = 0.031$) indicating faster RTs in the last than the first trials. No significant interactions emerged. In the external condition, the mean RTs were 433 (± 57) ms and 421 (± 46) ms (2.8% decrement) in the first and last trials, respectively; in the internal condition, the values were 499 (± 103) ms and 481 (± 82) ms (i.e., a decrement pairs to 3.7%) in the first and last trials, respectively.

In the fMRI experiments, analysis on accuracy did not yield significant results ($p > 0.1$; CE% = 1.38; Om% = 0.14), as well as that on the ICV ($p > 0.1$; 0.18 ± 0.07 and 0.16 ± 0.05 in internal and external condition, respectively). RTs were faster ($t_{13} = 3.20$; $p = 0.003$) in the external (596 ± 80 ms) than internal (628 ± 70 ms) condition. As found in the ERP experiment, we observed a main time-on-task effect ($F_{1,13} = 14.37$, $p = 0.002$), indicating faster RTs in the last than in the first trials. The interaction between condition and period was not significant. In the external condition, the mean RTs were 604 (± 55) ms and 593 (± 65) ms (1.8% decrement) in the first and last trials, respectively; in the internal condition, the values were 676 (± 105) ms and 635 (± 95) ms (i.e., a decrement pairs to 6.5%) in the first and last trials, respectively.

ANOVAs including the type of experiment (ERP and fMRI) as factor confirmed that participants were faster during the external (512 ± 13 ms) than the internal (462 ± 13 ms) condition ($F_{1,10} = 52.76$, $p < 0.0001$), but also revealed a strong speed-accuracy trade-off: participants were slower (RT: 612 ± 22 ms, $F_{1,10} = 28.27$, $p < 0.0001$) and more accurate (CE%: 1.38 ± 0.4; $F_{1,10} = 7.18$, $p = 0.018$) in fMRI than in ERP (RT: 463 ± 15 ms; CE%: 7.1 ± 2.0) experiment. The OM% and the ICV were not significant, as well as the interactions. The Levene's test for homogeneity of variance showed that, although the different number of trials, the groups (ERP and fMRI) were not different (internal: $F_{1,26} = 0.0008$, $p = 0.97$; external: $F_{1,26} = 2.283$, $p = 0.142$).

3.2. ERP results

3.2.1. External vs. Internal conditions

Fig. 2A shows the ERP waveforms for external (red lines) and internal (black lines) condition on the most relevant sites over bilateral prefrontal (Fp1 and Fp2), medial central (Cz) and bilateral occipital (O1 and O2) regions. Note that Go and No-go trials were averaged, providing very robust data (800 trials per subject). The activities in the preparation phase were clearly modulated by conditions. At occipital sites, the color change of fixation cross color (from white to green) evoked positive peaks from −2200 to −1600 ms, typical of cue-related visual activity (the P1 and P2 components); in the external condition, the occipital activity, in addition to the P1 and P2, showed 16 peaks evoked by the sequence of displayed circles (a sort of steady-state VEP across the entire interval before stimulus onset). The prefrontal slow rising negativity (the pN), starting at approximately 1600 ms before target onset in both conditions, became larger in the external than internal condition, especially on the left prefrontal site (Fp1), peaked at about 100 ms after stimulus onset and then rapidly decreased. The activity at the central sites (the CNV) started at approximately 1500 ms before stimulus onset in both conditions and became larger in the external than in the internal condition at about −300 ms, i.e. corresponding to the late CNV.

Topographical voltage mapping in the two time-windows is reported in Fig. 2B. Comparison of figures shows an enhanced widespread activity in the external condition during the earlier interval (shown on the left side of Fig. 2B). In the later interval (right side), the more large activity in the external condition was due to activities over prefrontal and central motor areas reflecting, according to an fMRI-guided ERP source analysis, the pN and the late CNV components, respectively. Cluster-based mass univariate analysis performed on the pre-stimulus ERP activity revealed significant amplitude differences between external and internal conditions (Fig. 2C). Activity was larger in external than in internal condition over a long period (in both intervals represented on the left and right side of Fig. 2C). The difference was significant starting at −1524 ms and extending up to stimulus onset (critical t value = ± 1.77, df = 13, test-wise $\alpha < 2 \times 10^{-5}$). This was due to the visual stimulation present in the foreperiod only in the external condition; indeed, the difference between conditions showed a posterior scalp distribution throughout the considered epoch (Fig. 2C) and moved to the frontal and central electrodes at about 200 ms before target onset.

3.2.2. Time on task effects

Particularly interesting is the within condition comparison contrasting first and last session quartile recordings, called first and last trials, respectively.

3.2.2.1. External condition. Fig. 3A shows the waveforms for the external condition superimposing first and last trials, respectively. The pN (at Fp1) and the occipital activity (at PO3 and PO4) were larger in the first than in the last trials. In contrast, the CNV did not change at all (see waveform at Cz). Topographical voltage mapping (Fig. 3B) in the two time-intervals (−1700/−1400 ms and −1400/0 ms) shows the time on task effect. In the early temporal window (left side), the effect was due to higher activity in parietal-occipital areas in the first trials; in the late temporal window (right side), activity was higher over prefrontal areas and parietal occipital areas in the first trials with respect to the last ones. Cluster-based mass univariate analysis (Fig. 3C) confirmed larger activity in the first trials (critical t value ± 2.16, df = 13, test-wise $\alpha < 2 \times 10^{-5}$), producing negative topographies on the maps. The inspection of the statistical *t*-test maps revealed that in a brief early time window (−1700/−1400 ms) this effect was present both at prefrontal and parietal-occipital electrodes, mainly in the left hemisphere, and extended over right scalp regions from −1400 ms to stimulus onset. The maps highlight statistical effects also over medial central sites, although not visible in the waveforms. Overall, the time on task produced a modest and diffuse reduction of cortical activity, as a sort of task learning.

3.2.2.2. Internal condition. In this condition, the time on task effect showed a pattern completely different from that observed in the external condition. Both the pN and the CNV were larger in the last than in the first trials (Fig. 4A), as also shown by the statistical maps (Fig. 4C). As in the case of the external task (but reversed in direction),

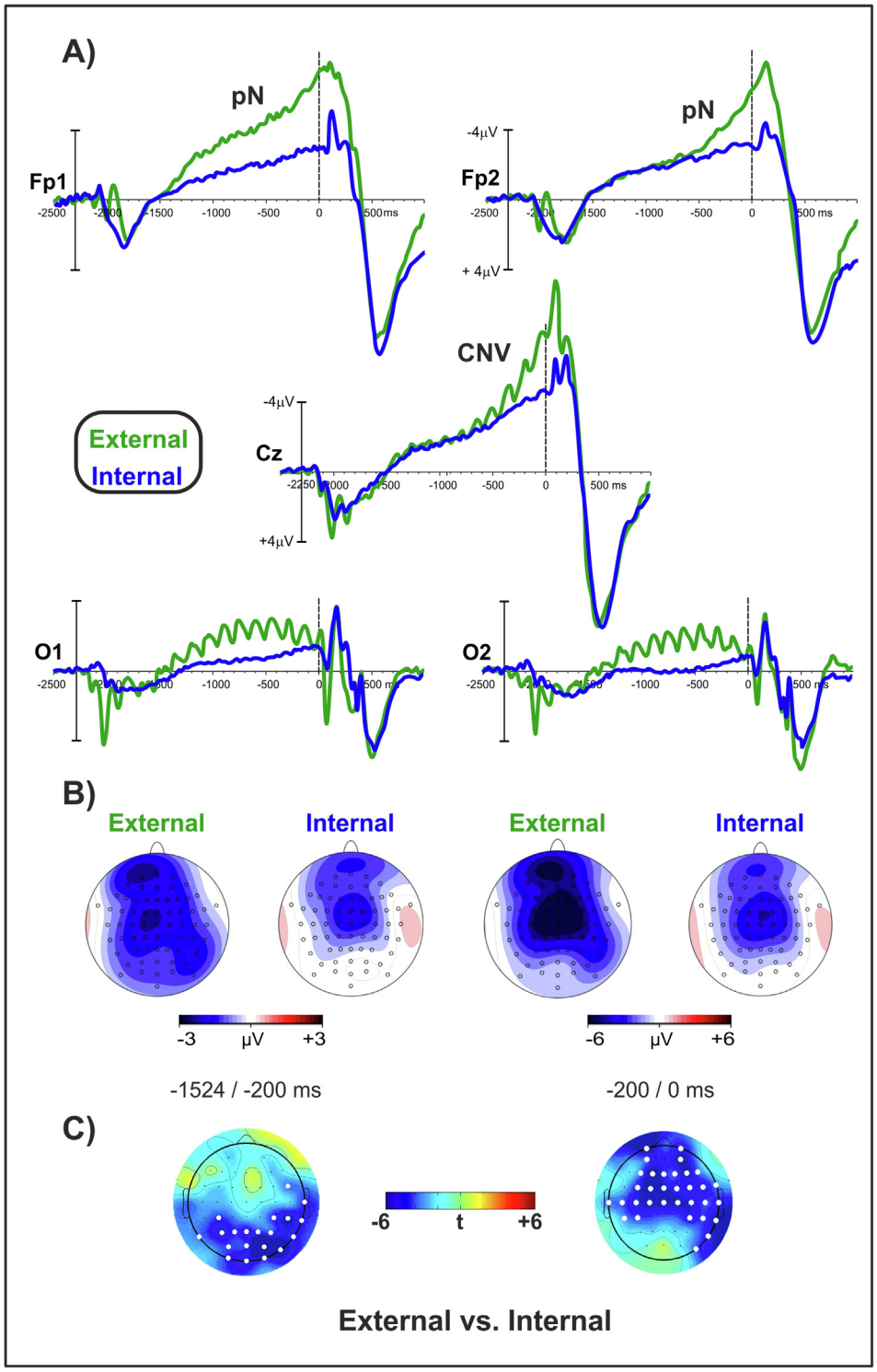

Fig. 2. (A) ERP waveforms for the external and internal conditions are represented by different colors. The time zero represents the stimulus onset. A value of −2250 ms on the horizontal axis corresponds with the onset of the warning stimulus. (B) Topographical mapping in the −1454/−200 ms and −200/0 ms intervals. (C) Cluster-based mass univariate analysis comparing external and internal conditions in the same time windows as the Panel B.

the time on task pN effect was more evident over the left hemisphere. Further, learning had limited or null effect on the small activity recorded over parietal-occipital sites. Topographical voltage mapping (Fig. 4B) indicated that in both considered intervals the effect was mainly due to larger activity after learning at prefrontal and frontal sites (corresponding, according to an fMRI-guided ERP source analysis, to the pN and CNV, respectively). Cluster-based mass univariate analysis (Fig. 4C) confirmed this pattern (critical t value = ± 2.16, df = 13, test-wise $\alpha < 2 \times 10^{-5}$). Statistical maps inspection revealed that the time on task effect was evident in two time-windows. The earlier time window (−1124/−1000 ms) showed a brief time on task effect over left prefrontal and medial frontal sites (consistent with earlier onset of the pN and the CNV component after learning); the later time window showed a sustained effect (−700/0 ms), involving bilateral prefrontal and medial frontal sites (consistent with larger amplitude of the pN and the CNV activities after learning).

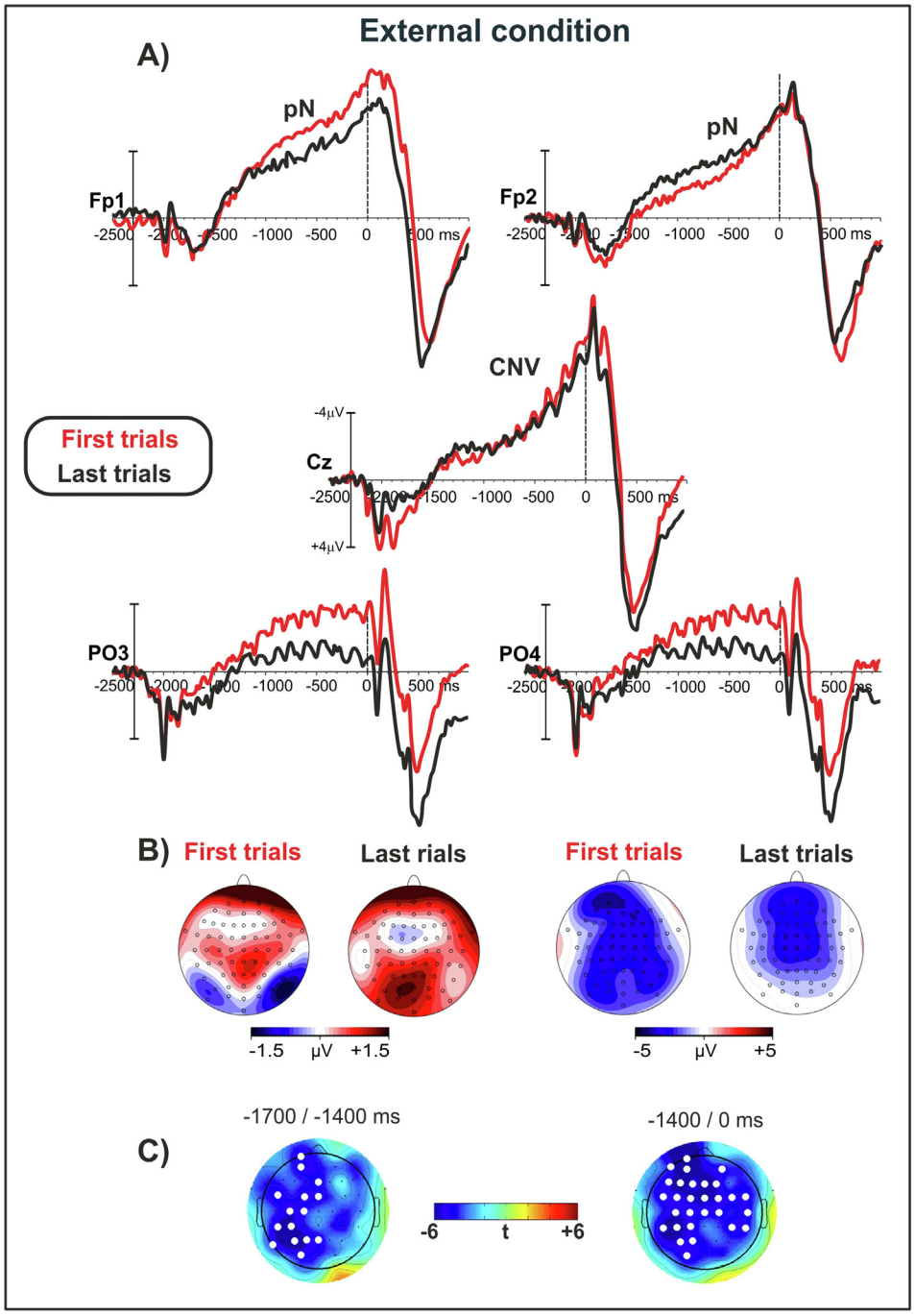

Fig. 3. (A) ERP waveforms for time on task effect in the external condition; different colors report first and last trials. A value of −2250 ms on the horizontal axis corresponds with the onset of the warning stimulus. (B) Topographical mapping in the −1700/−1400 ms and −1400/0 ms intervals. (C) Cluster-based mass univariate analysis comparing the first and the last quartile of trials.

For a direct visual comparison of the time on task effect between external and internal conditions, the grand-averaged waveforms of the first (Fig. 5A) and the last trials (Fig. 5B) in the two conditions are superimposed. The difference between conditions is very evident in the first trials, but barely present after learning. Only the pN (Fp1 and Fp2) and the CNV (Cz) components are shown. Overall, it seems that temporal orienting was immediately induced by external information; in contrast, processing reflecting temporal orienting emerged in the internal condition only after learning, when the informative value of the warning cue to predict the time of stimulus onset was effective.

3.3. fMRI results

3.3.1. Univariate results

Fig. 6 shows the "omnibus" F-contrast (any condition and task > Relax trial) revealing the involvement of a distributed network including the bilateral striate and extrastriate visual areas, the bilateral posterior intraparietal sulcus (pIPs), the bilateral horizontal segment of the intraparietal sulcus (hIPs), the left anterior intraparietal sulcus (aIPs) contralateral to the responding hand, the hand territory of the left primary motor and somatosensory areas (M1 and S1), and the bilateral supplementary and cingulate motor areas (SMA and CMA). Activations were also found in the anterior insula (aIns) and the adjacent

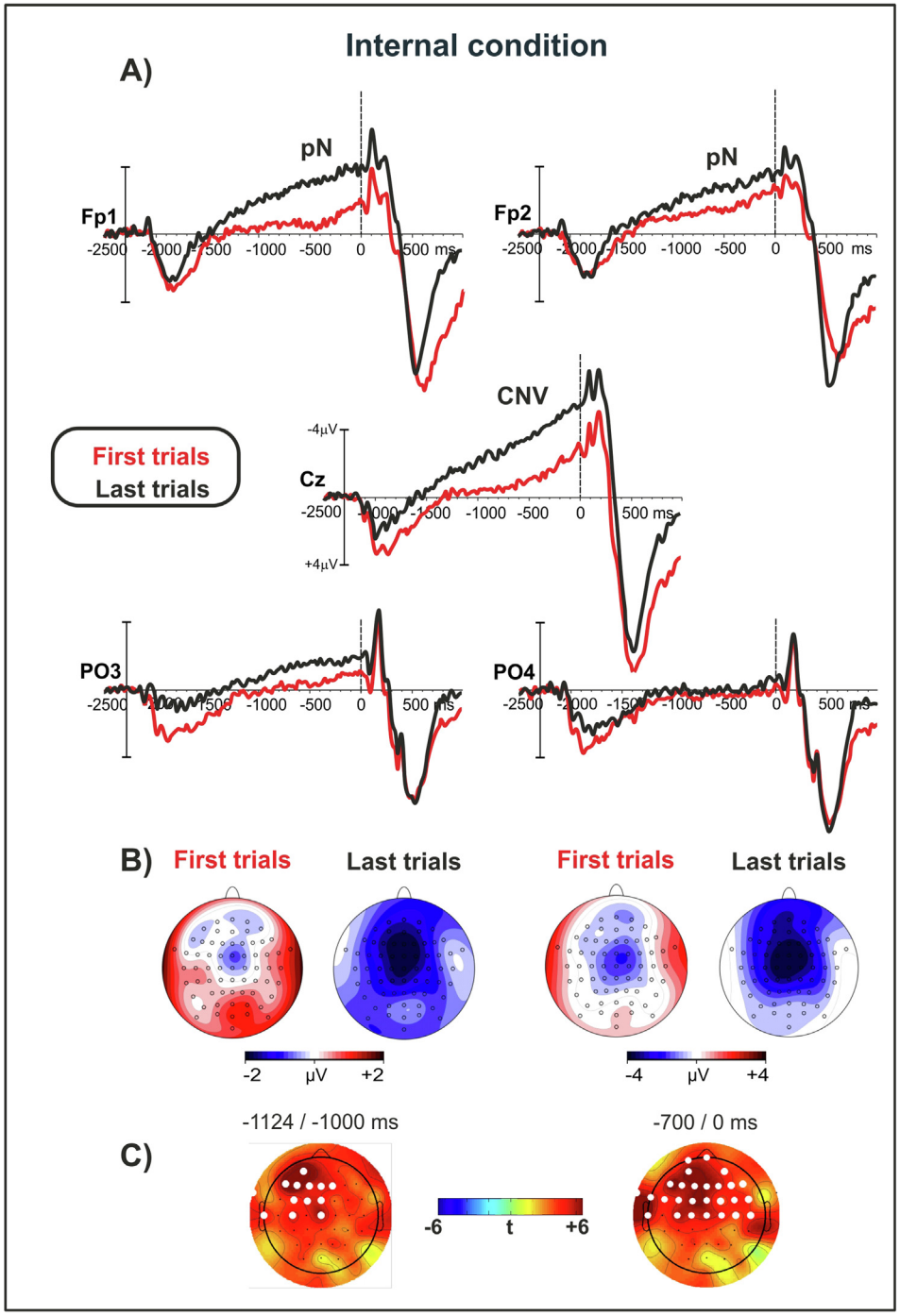

Fig. 4. (A) ERP waveforms for time on task effect in the internal conditions; different colors report first and last trials. A value of −2250 ms on the horizontal axis corresponds with the onset of the warning stimulus. (B) Topographical mapping in the −1124/−1000 ms and −700/0 ms intervals. (C) Cluster-based mass univariate analysis comparing the first and the last quartile of trials.

pars opercularis of the inferior frontal gyrus (iFg).

The anatomical location of local maxima (Talairach coordinates) in each of these brain regions is shown in Table 1.

ANOVA of the BOLD signal change estimated in each of the above-mentioned regions revealed that activations in left aIPs, striate and extrastriate visual areas were stronger in external than in internal condition. This is an obvious result, because visual stimulation during the foreperiod was present only in the external condition. The presence of motor response (Go trials) produced larger activity in the sensory-motor areas; moreover, Go trials were also associated to larger activation in the aIns and in the left aIPs respect on No-go trials.

Statistical results of these analyses are detailed in Table 2.

As for the effect of time on task, statistical analysis indicated that activation was higher in the first than the last trials. The general effect of condition (stronger activation in the external than internal condition) was replicated on this subset of data for the left aIPs and bilateral striate and extrastriate visual areas. No significant interactions were found in any region. Statistical results of this analysis are detailed in Table 3.

3.3.2. *Multivariate classification results*

We explored whether a linear classifier could correctly decode the external vs. internal condition from multi-voxel patterns of estimated

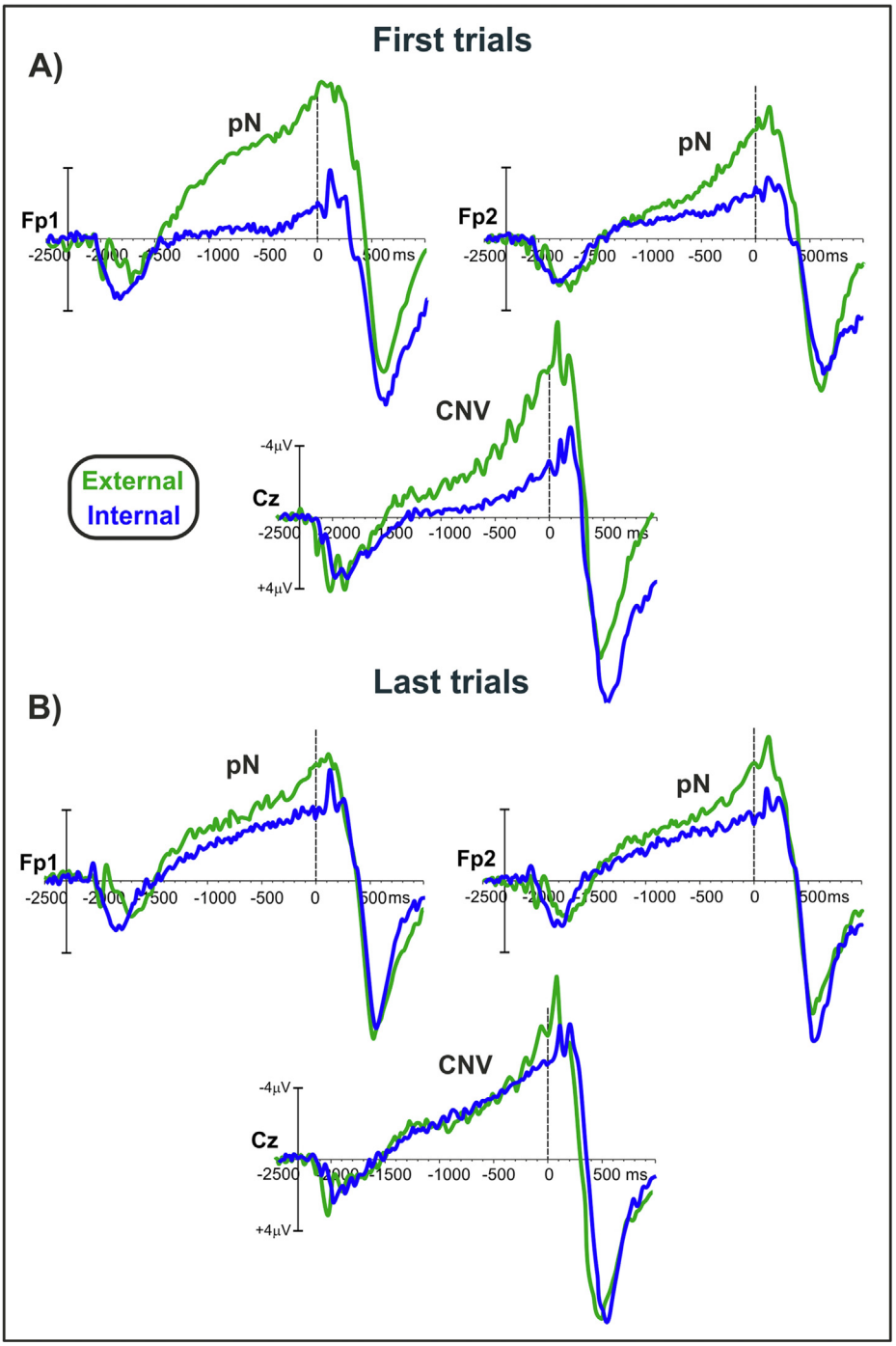

Fig. 5. Time on task effect: different effect for different conditions. (A) Before learning: overlap of ERP waveforms in the external (red lines) and internal (black lines) conditions. (B) After learning: overlap of ERP waveforms in the external (red lines) and internal (black lines) conditions. Waveforms are the same as in Figs. 3A and 4A, but arranged differently. (For interpretation of the references to color in this figure legend, the reader is referred to the web version of this article.)

neural activity. All the investigated regions allowed decoding the condition with above-change accuracy, except for the bilateral aIns and the right iFg. More information about decoding accuracy are detailed in Table 4.

3.4. ERP-fMRI combination

To associate the pre-stimulus ERPs to the found fMRI activations shown in Fig. 7, spatiotemporal BESA dipoles were seeded on the coordinates listed in Table 1. The choice of the coordinates to fit the dipoles was based on the fMRI activations, associating the coordinates found by fMRI to the time course of the EEG activation before stimulus onset. Further, we decided to fit only the dipoles likely generating the CNV (SMA + CMA) and the pN (iFg) components. We also included the extrastriate and the striate cortex to explain the occipital activation induced by the circles displayed in the foreperiod for the external condition. Dipole orientations were fitted in the −1300/0 ms and based on the source time-course intensity, the SMA-CMA areas and the bilateral iFg and extrastriate areas were the most active during the pre-stimulus phase. Due to their proximity, the SMA + CMA were represented by a single source. The resulting source time-course allowed to associate the iFg with the pN, the SMA-CMA with the CNV and the

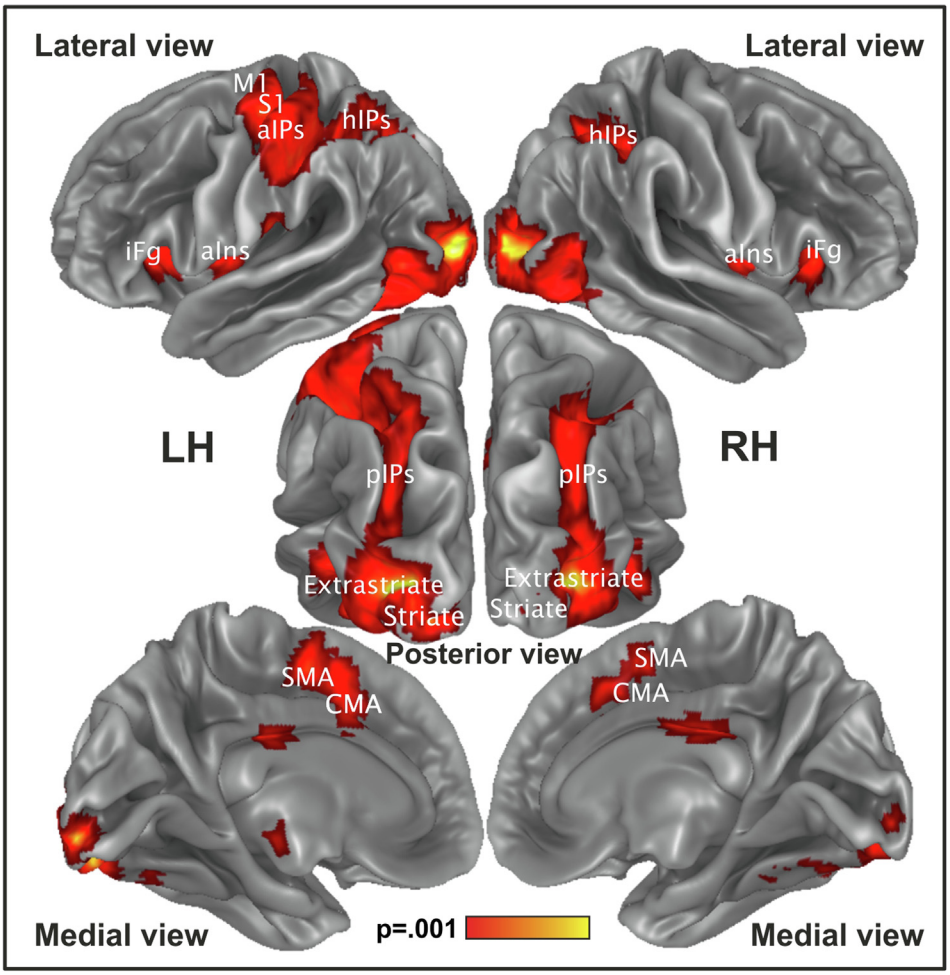

Fig. 6. fMRI results showing the network of brain area involved in the study (omnibus F-contrast). Activations are rendered on reconstructions of the lateral and mesial/posterior surfaces (top and bottom panels, respectively) of the two cerebral hemispheres of the Conte69 atlas. LH: Left Hemisphere; RH: Right Hemisphere.

Table 2
$F_{(1,13)}$ values of fMRI statistics ($p < 0.05$*, $p < 0.01$**). LH: Left Hemisphere; RH: Right Hemisphere.

Region	Hemisphere	Condition (external > internal)	Task (Go > No-go)	Interaction
M1/S1	LH	< 1	93.1**	< 1
aIPs	LH	6.0*	47.8**	< 1
SMA/CMA	LH	< 1	42.8**	< 1
	RH	< 1	15.0**	< 1
iFg	LH	< 1	10.4*	< 1
	RH	< 1	5.5*	< 1
aIns	LH	< 1	69.5**	< 1
	RH	< 1	41.2**	< 1
hIPs	LH	2.4	< 1	6.7*
	RH	< 1	< 1	3.4
pIPs	LH	6.2*	< 1	5.4*
	RH	2.0	< 1	2.2
Striate/Extrastriate	LH	80.0**	< 1	7.5*
	RH	78.4**	< 1	3.6

extrastriate areas with the parietal-occipital ERP activity. The residual variance of this 5-source model was 8.8% and 9.2% for the external and internal condition, respectively.

Fig. 7 shows the ERP based time-courses of activity in the mentioned fMRI regions for both internal and external conditions, separately for the two hemispheres. The earliest brain activity was detected in the bilateral iFg, starting with a slow rising negativity at approximately 1500–1600 ms prior to the stimulus onset and larger activity for the external condition. In both conditions, the SMA + CMA activities started approximately 1200 ms prior to the stimulus onset, slowly reached their negative peaks after stimulus onset and before the response; this activity was comparable in the two conditions. Striate and extrastriate areas were active in both conditions starting from −1800 ms, with an enhancement of activity depending on visual stimulation in the external condition. Note that ERP based time-courses of activity in fMRI-defined regions, in particular the ERP amplitude in the external/internal condition, is not completely consistent with results of ANOVA on the BOLD signal change. Similarities and differences between the two sets of data are discussed in the Discussion section.

Table 3
$F_{(1,13)}$ values of fMRI statistics for time-on-task effects (p < 0.05*, p < 0.01**). LH: Left Hemisphere; RH: Right Hemisphere.

Region	Hemisphere	Period (early > late)	Condition (external > internal)	Interaction
M1/S1	LH	39.2**	< 1	< 1
aIPs	LH	32.6**	6.3*	< 1
SMA/CMA	LH	16.1**	< 1	1.3
	RH	8.4*	< 1	1.8
iFg	LH	26.7**	< 1	3.6
	RH	24.7*	< 1	< 1
aIns	LH	13.0**	< 1	1.3
	RH	10.3**	< 1	< 1
hIPs	LH	10.9**	< 1	< 1
	RH	17.3**	< 1	1.8
pIPs	LH	21.9**	4.1	< 1
	RH	21.8**	2.4	< 1
Striate/Extrastriate	LH	15.7**	95.9**	< 1
	RH	26.9**	102.4**	3.6

Table 4
Multivariate classification results (p < 0.05*, p < 0.01**). LH: Left Hemisphere; RH: Right Hemisphere.

Region	Hemisphere	Classification Accuracy (Mean %)	*t*-test against chance (df 13)
M1/S1	LH	66%	6.9*
aIPs	LH	76%	6.6*
SMA/CMA	LH	68%	4.7*
	RH	68%	4.8*
iFg	LH	67%	5.9*
	RH	59%	3.1
aIns	LH	59%	2.3
	RH	54%	2.1
hIPs	LH	71%	6.8*
	RH	71%	5.4*
pIPs	LH	67%	4.4*
	RH	73%	5.5*
Striate/Extrastriate	LH	92%	11.5**
	RH	92%	12.1**

4. Discussion

The general aim of the study was to investigate brain preparation for speeded discriminative responses to stimuli in two temporal orienting conditions (called external and internal). To this aim, we studied how preparatory activities, and particularly the novel pN component, changed in the course of the experiment by means of the time on task effect and evaluated the effects of the external and internal conditions on both behavioral outcomes and cortical activities.

The use of fMRI and the dipole analysis allowed robust localization of the pN source, indicating similar origin in the two conditions within the iFg, and confirming previous ERP/fMRI studies on the pN source (Di Russo et al., 2016; Ragazzoni et al., 2019; Sulpizio et al., 2017). The amplitudes of the scalp-recorded activities over prefrontal (the pN component) and premotor (the CNV component) regions were larger in the external than in the internal condition; thus, temporal predictability, strongly induced by the external condition, affected the analyzed components, with larger effect at prefrontal sites. This result supports the view that the pN may reflect processing related to temporal orienting, as already proposed for the CNV.

A growing negative activity on bilateral occipital cortices was also found. Although larger in the external than in the internal condition, because of the phasic response to the circles displayed in the foreperiod in the former condition, this growing activity was also present in the latter condition, where no visual stimuli were displayed. Such an anticipatory activity, previously called visual negativity (vN) and reported in several visual tasks (as the Go/No-go, simple response tasks and passive vision), was related to sensory readiness (Bianco et al., 2019; Di Russo et al., 2019). Present data confirm the multicomponential nature of the proactive control in visual-motor tasks, which involves premotor, prefrontal and, also, occipital brain areas (Bianco et al., 2019; Di Russo et al., 2019; Jennings, Van der Molen, & Steinhauer, 1998; Ruchkin, Canoune, Johnson, & Ritter, 1995; van Boxtel, 1994).

We believe that the results about the time on task effect in the two conditions are particularly interesting. The effect of learning in the external condition was limited; this was expected since the characteristics of the external condition were designed to immediately induce temporal orienting. The pN and the vN components showed a modest, not significant, amplitude reduction in the last trials; further, the onset and the amplitude of the CNV component recorded in the first and in the last trials were comparable. At behavioral level, the RTs were faster after learning by 2.7%. Thus, faster RTs were associated with a slightly reduced cortical activity. These results are consistent with the observation that experience reduces the amount of resources needed for the performance during the preparation stage (Mento & Valenza, 2016), and with the more general view of higher neural efficiency in expert subjects, i.e., good performance obtained at lower cortical cost (Berchicci, Quinzi, Dainese, & Di Russo, 2017).

By contrast, the effect of learning was large in the internal condition: in the first trials the pN and the CNV started later and were lower in amplitude compared to the last trials. In the last trials, the participants had learned (likely based on both intentional and unintentional orienting mechanisms; Los & Heslenfeld, 2005) the temporal information conveyed by the cue, and we propose that the longer and enhanced preparation activity at both prefrontal and premotor level supports effective temporal orienting; consistently, RTs in the last trials were faster (by 3.6%) than RTs measured before learning. Thus, in the internal condition, faster RTs were recorded after learning at the cost of a relevant increment of cortical activity. Interestingly, after learning (i.e., last trials; Fig. 5, panel B) the pN and the CNV components recorded in internal and external conditions had comparable amplitude and were associated with their best RTs (still showing 60 ms advantage for the external condition; the advantage was of 66 ms before learning).

Overall, we propose that the proactive cognitive control reflected by the prefrontal component pN (Berchicci et al., 2012, 2016; Bianco et al., 2017; Di Russo et al., 2016) may also include temporal orienting processes, in line with previous data on the CNV, reflecting both time orienting and motor preparation (Los & Heslenfeld, 2005; Macar & Vidal, 2003; Macar et al., 1999; Mento & Vallesi, 2016; Mento et al., 2013, 2015; Monfort et al., 2000; Pfeuty et al., 2003, 2005; Trillenberg et al., 2000).

Previous scalp recordings showed a positive polarity (instead of negative) at prefrontal leads for the external condition (Berchicci et al., 2015); this could suggest that sources at prefrontal level were different than the internal condition. Present fMRI data allow excluding this hypothesis; moreover, the polarity inversion of the pN was not replicated in the present study, possibly because we used long and

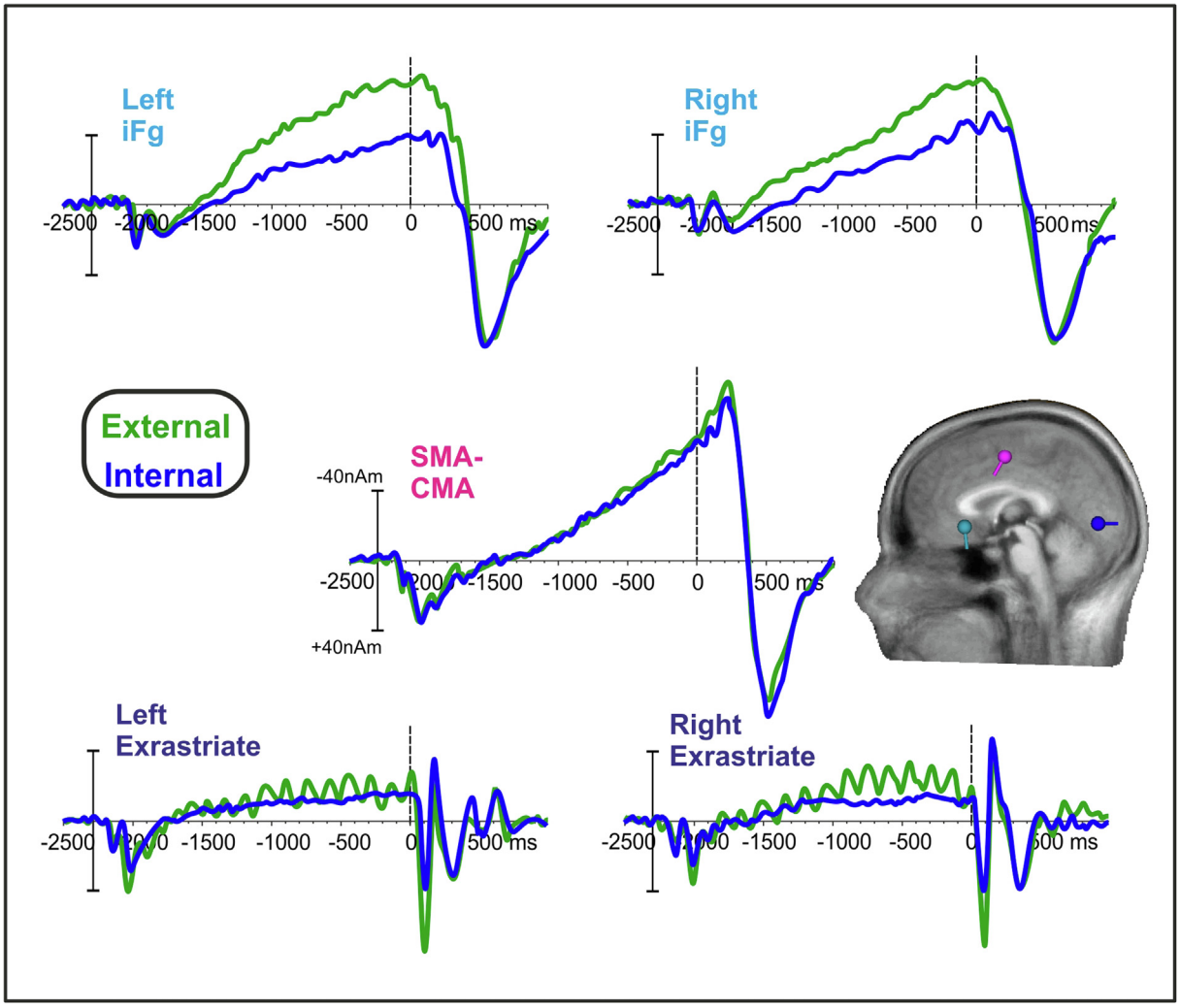

Fig. 7. fMRI-guided spatiotemporal source analysis of pre-stimulus ERP activity in the two conditions (indicated by different colors). Dipoles were seeded over bilateral inferior Frontal gyrus (iFg), extrastriate visual cortex, while a single dipole represent the medial Supplementary and Cingulate motor areas (SMA-CMA) as shown in the fMRI template. Source time-course in the internal and external conditions is overlapped.

variable stimulus-onset asynchrony (whereas the ISI was fixed), and a different baseline. In any case, present fMRI findings support the hypothesis that bilateral iFg is the source of the pN component in both external and internal conditions.

fMRI data and, particularly, similarities and differences between present ERPs and fMRI data deserve a specific comment. fMRI showed stronger activity of left aIPs, striate and extrastriate visual areas in external than in internal condition; these results are consistent with scalp recordings at occipital-parietal leads and are an obvious consequence of the visual stimulation in the foreperiod present only in the external condition. The higher activity of left aIPS confirms previous findings showing that the left inferior parietal lobe (IPL) is preferentially activated by cueing time-predictable tasks (Coull, Vidal, & Burle, 2016), and is consistent with the electrophysiological left hemisphere dominance in external condition detected by cluster-based mass univariate analysis. Brain imaging studies using predictable foreperiods (Sakai et al., 2000) and temporally informative cues (Coull & Nobre, 1998; Coull, Frith, Buchel, & Nobre, 2000) showed the engagement of inferior parietal and premotor brain regions (Nobre et al., 2007). Temporal orienting task selectively activated the left parietal cortex when participants used temporal cues to enhance perceptual discriminations or to speed motor responses (Davranche, Nazarian, Vidal, & Coull, 2011). The neural network involved in temporal orienting selectively comprises the left parietal cortex, centered around the IPS, regardless of the effector (eyes or hands), the side (left or right) required for the response (Coull et al., 2000, 2011; Coull & Nobre, 1998), and the proportion or motor nature of the task (Cotti, Rohenkohl, Stokes, Nobre, & Coull, 2011; Davranche et al., 2011). Other studies have linked the temporal predictability to right-lateralized prefrontal and parietal cortex (Bueti, Bahrami, Walsh, & Rees, 2010; Vallesi et al., 2007, 2009); however, these studies manipulated the hazard function, which is quite different from the present experimental paradigm. According to other temporal orienting studies (Cotti et al., 2011; Coull et al., 2000, 2011; Triviño, Correa, Arnedo, & Lupiáñez, 2010), right-sided cortical activation would mark temporal prediction as an updating of the time passing, whereas left-sided regions are active when a fixed temporal prediction is used. Present data support this latter hypothesis since no specific right-sided activation was detected. Overall, the pivotal role played by left pIPS in temporal orienting when external visual cues are provided was confirmed by fMRI data and its involvement was also detected by ERPs (see external condition, first vs. last trials; Fig. 3, panels B and C).

On the other hand, fMRI and ERP techniques produced different results as it regards the effect of conditions on the activity recorded in CMA-SMA and iFg regions. fMRI data from univariate analysis did not show the effect of condition for both the CMA/SMA and the iFg; this result contrasts with the amplitude by condition modulation measured by scalp recording. However, fMRI data from MVPA indicated that

distinct patterns of neural activity were observed in the bilateral CMA/SMA and in the left iFg, indicating that these regions contain enough information to discriminate between external and internal conditions. The difference between fMRI and ERP data is evident for the time on task effect. fMRI showed higher activation in the first trials of the experiment than the last trials in all regions of interest (including iFg and CMA-SMA) in both conditions. This result is consistent with fMRI studies of time on task effect typically observed in vigilance tasks (for a review see Warm, Parasuraman, & Matthews, 2008), showing a decrease in neural activation and regional blood flow as one is engaged in a task over time. At electrophysiological level, a similar effect was observed for the pN and the CNV components in the external condition, but not in the internal condition (where the direction of the effect was opposite). The explanation of the lack of coherence between results obtained with the two techniques is difficult and subject to caveats (e.g., Dale & Halgren, 2001; Rosa, Daunizeau, & Friston, 2010). In addition, the ERP always preceded the fMRI experiment, and this fixed order might affect the time on task effect in the fMRI experiment. One can also assume that the different number of trials between ERP and fMRI paradigms could have induced different learning effect. Indeed, if the participants have performed 200 trials from the first to the last trials in ERPs, in fMRI they performed only 36 trials. The low trials number in fMRI may have not induced a pure learning effect for the internal condition. All these reasons require caution in interpreting the comparison between results obtained with the two techniques. Also, the assumption that hemodynamic response obtained with fMRI is driven by the same neural activity that gives rise to the ERP may be questioned (e.g., Bonmassar et al., 2001; Di Russo & Pitzalis, 2013; Di Russo et al., 2016, Heinze et al., 1994; Snyder, Abdullaev, Posner, & Raichle, 1995; Sulpizio et al., 2017); such a correspondence (investigated for visual ERPs) appears to be optimal for human medial occipital cortex (and present study confirms this correspondence), but it is less robust for other areas (Gratton, Goodman-Wood, & Fabiani, 2001). Therefore, differences between ERP and fMRI data could be due to intrinsic characteristics of the two techniques.

As regards the behavioral level, RTs in the external condition were faster than internal condition in both fMRI and ERP experiments. The advantage of external condition is in line with previous results (Correa & Nobre, 2008). One may note that RTs were faster and accuracy was lower in ERP than fMRI experiments. This outcome is consistent with speed-accuracy trade-off (Bogacz, Wagenmakers, Forstmann, & Nieuwenhuis, 2010). The task instructions were identical for the two experiments; physical characteristics of the stimuli (contrast and luminance) were the same; whereas body position of the subjects (seated on a chair in the ERP and lying on their back in the fMRI with movements limited by scanner constraints), number of trials (400 and 72 Go trials in ERP and fMRI, respectively, for each task) and body segment used to respond (right index finger and right hand in the ERP and fMRI, respectively) differed. These latter factors may be responsible for the different absolute values of RTs in ERP and fMRI experiments.

We must acknowledge a study limitation and related future perspectives. The external condition involved visual inputs (i.e., the flashed circles), which were not present in the internal condition. Data in Fig. 2 show that visual processing of this input also influences central electrodes (as shown by small oscillatory signals related to the circles presentation sequence). One may argue that the enhanced CNV amplitude in the external condition may be driven by this occipital activity; however, this hypothesis could account for the results in the early time window only, not for the effect in the late time window. Moreover, the result of very similar activities recorded at prefrontal and central electrodes after learning in internal (where visual stimulation is absent) and external (where stimulation is present) condition does not support this hypothesis. In any case, to provide support for the present results' interpretation, a future study will introduce a control condition in which the same circles are presented in the foreperiod, but displayed randomly, i.e., not providing information about the time of stimulus onset.

In conclusion, present data show that the pN component reflects also temporal orienting, as already shown for the CNV component. Data confirm that the iFg was the source of the pN component, and that the sources of the pN and the CNV are distinct.

5. Compliance with Ethical standards

All procedures performed in the study involved human participants and all procedures were reviewed and approved by the Santa Lucia Foundation Ethical Committee.

Funding

The work was supported by the University of Foro Italico (grant number RIC162015) to Francesco Di Russo.

Ethical approval

All participants gave their informed consent according to 1964 Helsinki declaration and its later amendments or comparable ethical standards.

Informed consent

Informed consent was obtained from all individual participants included in the study.

CRediT authorship contribution statement

Marika Berchicci: Conceptualization, Methodology, Software, Formal analysis, Investigation, Resources, Data curation, Writing - original draft, Writing - review & editing, Visualization. **Valentina Sulpizio:** Conceptualization, Methodology, Software, Formal analysis, Investigation, Resources, Data curation, Writing - original draft, Writing - review & editing, Visualization. **Giovanni Mento:** Methodology, Software, Formal analysis, Data curation, Writing - original draft, Writing - review & editing. **Giuliana Lucci:** Methodology, Investigation, Writing - original draft, Writing - review & editing. **Nicole Civale:** Investigation. **Gaspare Galati:** Conceptualization, Methodology, Writing - original draft, Writing - review & editing. **Sabrina Pitzalis:** Conceptualization, Methodology, Formal analysis, Writing - original draft, Writing - review & editing. **Donatella Spinelli:** Conceptualization, Methodology, Writing - original draft, Writing - review & editing. **Francesco Di Russo:** Conceptualization, Methodology, Formal analysis, Writing - original draft, Writing - review & editing, Writing - original draft, Writing - review & editing.

Declaration of Competing Interest

The authors declare that they have no known competing financial interests or personal relationships that could have appeared to influence the work reported in this paper.

Appendix A. Supplementary material

Supplementary data to this article can be found online at https://doi.org/10.1016/j.bandc.2020.105565.

References

Aron, A. R., & Poldrack, R. A. (2006). Cortical and subcortical contributions to stop signal response inhibition: Role of the subthalamic nucleus. *Journal of Neuroscience, 26*, 2424–2433.

Aron, A. R. (2011). From reactive to proactive and selective control: Developing a richer model for stopping inappropriate responses. *Biological Psychiatry, 69*(12), e55–e68.

Berchicci, M., Lucci, G., & Di Russo, F. (2013). The benefits of physical exercise on the aging brain: The role of the prefrontal cortex. *Journals of Gerontology Series A: Biological Sciences and Medical Sciences*. https://doi.org/10.1093/gerona/glt094.

Berchicci, M., Lucci, G., Perri, R. L., Spinelli, D., & Di Russo, F. (2014). Benefits of physical exercise on basic visuo-motor functions across age. *Frontiers in Aging Neuroscience*. https://doi.org/10.3389/fnagi.2014.00048.

Berchicci, M., Lucci, G., Pesce, C., Spinelli, D., & Di Russo, F. (2012). Prefrontal hyperactivity in older people during motor planning. *NeuroImage, 62*, 1750–1760.

Berchicci, M., Lucci, G., Spinelli, D., & Di Russo, F. (2015). Stimulus onset predictability modulates proactive action control in a Go/No-go task. *Frontiers in Behavioral Neuroscience, 9*, 101. https://doi.org/10.3389/fnbeh.2015.00101.

Berchicci, M., Quinzi, F., Dainese, A., & Di Russo, F. (2017). Time-source of neural plasticity in complex bimanual coordinative tasks: Juggling. *Behavioral Brain Research, 328*, 87–94.

Berchicci, M., Spinelli, D., & Di Russo, F. (2016). New insights about old waves. Stimulus- and response-locked ERPs on the same time-window. *Biological Psychology, 117*, 202–215.

Berchicci, M., Ten Brink, A. F., Quinzi, F., Perri, R. L., Spinelli, D., & Di Russo, F. (2019). Electrophysiological evidence of sustained spatial attention effects over anterior cortex: Possible contribution of the anterior insula. *Psychophysiology,* e13369.

Bianco, V., Berchicci, M., Perri, R. L., Spinelli, D., & Di Russo, F. (2017). The proactive self-control of actions: Time-course of underlying brain activities. *NeuroImage, 156*, 388–393.

Bianco, V., Perri, R. L., Berchicci, M., Quinzi, F., Spinelli, D., & Di Russo, F. (2019). Modality-specific sensory readiness for upcoming events revealed by slow cortical potentials. *Brain Structure and Function*. https://doi.org/10.1007/s00429-019-01993-8.

Bledowski, C., Kadosh, K. C., Wibral, M., Rahm, B., Bittner, R. A., Hoechstetter, K., et al. (2006). Mental chronometry of working memory retrieval: A combined functional magnetic resonance imaging and event-related potentials approach. *Journal of Neuroscience, 26*(3), 821–829.

Boccia, M., Piccardi, L., Palermo, L., Nemmi, F., Sulpizio, V., Galati, G., et al. (2014). A penny for your thoughts! Patterns of fMRI activity reveal the content and the spatial topography of visual mental images. *Human Brain Mapping, 36*, 945–958.

Boccia, M., Sulpizio, V., Palermo, L., Piccardi, L., Guariglia, C., & Galati, G. (2016). I can see where you would be: Patterns of fMRI activity reveal imagined landmarks. *NeuroImage, 144*, 174–182.

Bogacz, R., Wagenmakers, E. J., Forstmann, B. U., & Nieuwenhuis, S. (2010). The neural basis of the speed and accuracy tradeoff. *Trends in Neuroscience, 33*, 10–16.

Bonmassar, G., Schwartz, D. P., Liu, A. K., Kwong, K. K., Dale, A. M., & Belliveau, J. W. (2001). Spatiotemporal brain imaging of visual-evoked activity using interleaved EEG and fMRI recordings. *NeuroImage, 13*, 1035–1043.

Boynton, G. M., Engel, S. A., Glover, G. H., & Heeger, D. J. (1996). Linear systems analysis of functional magnetic resonance imaging in human V1. *Journal of Neuroscience, 1613*, 4207–4221.

Brass, M., & von Cramon, D. Y. (2002). The role of the frontal cortex in task preparation. *Cerebral Cortex, 12*, 908–914.

Braver, T. S., Paxton, J. L., Locke, H. S., & Barch, D. M. (2009). Flexible neural mechanisms of cognitive control within human prefrontal cortex. *Proceedings of the National Academy of Sciences, 106*(18), 7351–7356.

Brunia, C. H. M., & Damen, E. J. P. (1988). Distribution of slow brain potentials related to motor preparation and stimulus anticipation in a time estimation task. *Electroencephalography and Clinical Neurophysiology, 69*, 234–243.

Brunia, C. H. M., van Boxtel, G. J. M., & Böcker, K. B. E. (2011). Negative Slow Waves as Indices of Anticipation: The Bereitschaftspotential, the Contingent Negative Variation, and the Stimulus-Preceding Negativity. In E. S. Kappenman, & S. J. Luck (Eds.). *The Oxford Handbook of Event-Related Potential Components* (pp. 242–263). Oxford: Oxford University Press. https://doi.org/10.1093/oxfordhb/9780195374148.013.0108.

Brunia, C. H. M. (1988). Movement and stimulus preceding negativity. *Biological Psychology, 26*, 165–178.

Bueti, D., Bahrami, B., Walsh, V., & Rees, G. (2010). Encoding of temporal probabilities in the human brain. *The Journal of Neuroscience, 30*, 4343–4352.

Carlson, J. M., Foti, D., Mujica-Parodi, L. R., Harmon-Jones, E., & Hajcak, G. (2011). Ventral striatal and medial prefrontal BOLD activation is correlated with reward-related electrocortical activity: A combined ERP and fMRI study. *Neuroimage, 57*(4), 1608–1616.

Chikazoe, J., Jimura, K., Hirose, S., Yamashita, K., Miyashita, Y., & Konishi, S. (2009). Preparation to inhibit a response complements response inhibition during performance of a stop-signal task. *The Journal of Neuroscience, 29*(50), 15870–15877.

Correa, A., & Nobre, A. C. (2008). Neural modulation by regularity and passage of time. *Journal of Neurophysiology, 100*(3), 1649–1655.

Correa, A., Triviño, M., Pérez-Dueñas, C., Acosta, A., & Lupiáñez, J. (2010). Temporal preparation, response inhibition and impulsivity. *Brain and Cognition, 73*, 222–228.

Cotti, J., Rohenkohl, G., Stokes, M., Nobre, A. C., & Coull, J. T. (2011). Functionally dissociating temporal and motor components of response preparation in left intraparietal sulcus. *NeuroImage, 54*(2), 1221–1230.

Coull, J. T., & Nobre, A. C. (1998). Where and when to pay attention: The neural systems for directing attention to spatial locations and to time intervals as revealed by both PET and fMRI. *Journal of Neuroscience, 18*, 7426–7435.

Coull, J. T., Cheng, R. K., & Meck, W. H. (2011). Neuroanatomical and neurochemical substrates of timing. *Neuropsychopharmacology: Official Publication of the American College of Neuropsychopharmacology, 36*(1), 3–25.

Coull, J. T., Frith, C. D., Buchel, C., & Nobre, A. C. (2000). Orienting attention in time: Behavioural and neuroanatomical distinction between exogenous and endogenous shifts. *Neuropsychologia, 38*, 808–819.

Coull, J. T., Vidal, F., & Burle, B. (2016). When to act, or not to act: That's the SMA's question. *Current Opinion in Behavioral Sciences*. https://doi.org/10.1016/j.cobeha.2016.01.003.

Criaud, M., & Boulinguez, P. (2013). Have we been asking the right questions when assessing response inhibition in go/no-go tasks with fMRI? A meta-analysis and critical review. *Neuroscience and Biobehavioral Reviews, 371*, 11–23.

Crottaz-Herbette, S., & Menon, V. (2006). Where and when the anterior cingulate cortex modulates attentional response: Combined fMRI and ERP evidence. *Journal of Cognitive Neuroscience, 18*(5), 766–780.

Cunnington, R., Iansek, R., Bradshaw, J. L., & Phillips, J. G. (1995). Movement-related potentials in Parkinson's disease: Presence and predictability of temporal and spatial cues. *Brain, 118*, 935–950.

Dale, A. M., & Halgren, E. (2001). Spatiotemporal mapping of brain activity by integration of multiple imaging modalities. *Current Opinion in Neurobiology, 11*, 202–208.

Davranche, K., Nazarian, B., Vidal, F., & Coull, J. T. (2011). Orienting attention in time activates left intraparietal sulcus for perceptual and motor task goals. *Journal of Cognitive Neuroscience, 23*, 3318–3330.

Di Russo, F., Berchicci, M., Bianco, V., Perri, R. L., Pitzalis, S., Quinzi, F., et al. (2019). Normative Event-Related Potentials from sensory and cognitive tasks reveal occipital and frontal activities prior and following visual events. *NeuroImage, 196*, 173–187.

Di Russo, F., Berchicci, M., Bozzacchi, C., Perri, R. L., Pitzalis, S., & Spinelli, D. (2017). Beyond the "Bereitschaftpotential": Action preparation behind cognitive functions. *Neuroscience & Biobehavioral Reviews*. https://doi.org/10.1016/j.neubiorev.2017.04.019.

Di Russo, F., Incoccia, C., Formisano, R., Sabatini, U., & Zoccolotti, P. (2005). Abnormal motor preparation in severe traumatic brain injury with good recovery. *Journal of Neurotrauma, 22*(2), 297–312.

Di Russo, F., Lucci, G., Sulpizio, V., Berchicci, M., Spinelli, D., Pitzalis, S., et al. (2016). Spatiotemporal brain mapping of the preparation, perception and action phases. *NeuroImage*. https://doi.org/10.1016/j.neuroimage.2015.11.036.

Di Russo, F., & Pitzalis, S. (2013). EEG-fMRI combination for the study of visual perception and spatial attention. *Cognitive electrophysiology of attention: Signals of the mind* (pp. 58–70). Academic Press.

Frank, M. J. (2006). Hold your horses: A dynamic computational role for the subthalamic nucleus in decision making. *Neural Network, 19*(8), 1120–1136.

Friston, K. J., Fletcher, P., Josephs, O., Holmes, A., Rugg, M. D., et al. (1998). Event-related fMRI: Characterizing differential responses. *NeuroImage, 7*, 30–40.

Galati, G., Committeri, G., Spitoni, G., Aprile, T., Di Russo, F., Pitzalis, S., et al. (2008). A selective representation of the meaning of actions in the auditory mirror system. *Neuroimage, 40*, 1274–1286.

Gillies, A. J., & Willshaw, D. J. (1998). A massively connected subthalamic nucleus leads to the generation of widespread pulses. *Proceedings of the Royal Society of London B: Biological Sciences, 265*(1410), 2101–2109.

Gómez, C. M., Flores, A., & Ledesma, A. (2007). Fronto-parietal networks activation during the contingent negative variation period. *Brain Research Bulletin, 73*, 40–47.

Gómez, C. M., Marco, J., & Grau, C. (2003). Preparatory visuo-motor cortical network of the contingent negative variation estimated by current density. *Neuroimage, 20*, 216–224.

Gonçalves, F. G., Rego, G., Conde, T., Leite, G., Carvalho, S., Lapenta, O. M., et al. (2018). Mind Wandering and Task-Focused Attention: ERP Correlates. *Scientific Reports, 8*(1), 7608.

Gratton, G., Goodman-Wood, M. R., & Fabiani, M. (2001). Comparison of neuronal and hemodynamic measures of the brain response to visual stimulation: An optical imaging study. *Human Brain Mapping, 13*, 13–25.

Groppe, D. M., Urbach, T. P., & Kutas, M. (2011). Mass univariate analysis of event-related brain potentials/fields I: A critical tutorial review. *Psychophysiology,* 1–15.

Hampshire, A., Chamberlain, S. R., Monti, M. M., Duncan, J., & Owen, A. M. (2010). The role of the right inferior frontal gyrus: Inhibition and attentional control. *Neuroimage, 50*(3), 1313–1319.

Heinze, H. J., Mangun, G. R., Burchert, W., Hinrichs, H., Scholz, M., Munte, T. F., et al. (1994). Combined spatial and temporal imaging of spatial selective attention in humans. *Nature, 392*, 543–546.

Hoffmann, S., Borges, U., Broker, L., Labored, S., Liepelt, R., Lobinger, B. H., et al. (2018). The psychophysiology of action: A multidisciplinary endeavor for integrating action and cognition. *Frontiers in Psychology, 9*, 1432.

Jahanshahi, M., Jenkins, I. H., Brown, R. G., Marsden, C. D., Passingham, R. E., & Brooks, D. J. (1995). Self-initiated versus externally triggered movements. *Brain, 118*(4), 913–933.

Jamadar, S., Hughes, M., Fulham, W. R., Michie, P. T., & Karayanidis, F. (2010). The spatial and temporal dynamics of anticipatory preparation and response inhibition in task-switching. *Neuroimage, 51*, 432–449.

Jenkins, I. H., Jahanshahi, M., Jueptner, M., Passingham, R. E., & Brooks, D. J. (2000). Self-initiated versus externally triggered movements. *Brain, 123*(6), 1216–1228.

Jennings, J. R., Van der Molen, M. W., & Steinhauer, S. R. (1998). Preparing the heart, eye, and brain: Foreperiod length effects in a nonaging paradigm. *Psychophysiology, 35*, 90–98.

Jung, T. P., Makeig, S., Humphries, C., Lee, T. W., Mckeown, M. J., Iragui, V., et al. (2000). Removing electroencephalographic artifacts by blind source separation. *Psychophysiology, 37*, 163–178.

Kornhuber, H. H., & Deecke, L. (1965). Changes in the brain potential in voluntary movements and passive movements in man: Readiness potential and reafferent potentials. *Pflugers Archiv fur die gesamte Physiologie des Menschen und der Tiere, 284*, 1–17.

Kwong, K. K., Belliveau, J. W., Chesler, D. A., Goldberg, I. E., Weisskoff, R. M., Poncelet, B. P., et al. (1992). Dynamic magnetic resonance imaging of human brain activity during primary sensory stimulation. *Proceedings of the National Academy of Sciences of*

the United States of America, 8912, 5675–5679.
Los, S. A., & Heslenfeld, D. J. (2005). Intentional and unintentional contributions to nonspecific preparation: Electrophysiological evidence. *Journal of Experimental Psychology: General, 134*, 52–72.
Lucci, G., Berchicci, M., Perri, R. L., Spinelli, D., & Di Russo, F. (2016). Effect of target probability on pre-stimulus brain activity. *Neuroscience, 322*, 121–128.
Macar, F., & Vidal, F. (2003). The CNV peak: An index of decision making and temporal memory. *Psychophysiology, 40*, 950–954.
Macar, F., Vidal, F., & Casini, L. (1999). The supplementary motor area in motor and sensory timing: Evidence from slow brain potential changes. *Experimental Brain Research, 125*, 271–280.
MacDonald, A. W., III, Cohen, J. D., Stenger, V. A., & Carter, C. S. (2000). Dissociating the role of the dorsolateral prefrontal and anterior cingulate cortex in cognitive control. *Science, 288*, 1835–1838.
Mazziotta, J. C., Toga, A. W., Evans, A., Fox, P., & Lancaster, J. (1995). A probabilistic atlas of the human brain: Theory and rationale for its development. The International Consortium for Brain Mapping ICBM. *NeuroImage, 2*, 89–101.
Mento, G., & Valenza, E. (2016). Spatiotemporal neurodynamics of automatic temporal expectancy in 9-month old infants. *Scientific Reports, 6*(1), 36525.
Mento, G., & Vallesi, A. (2016). Spatiotemporally dissociable neural signatures for generating and updating expectation over time in children: A High Density-ERP study. *Developmental Cognitive Neuroscience, 19*, 98–106.
Mento, G., Tarantino, V., Sario, M., & Bisiacchi, S. (2013). Automatic temporal expectancy: A high-density event-related potential study. *PLOS one, 8*(5), e62896.
Mento, G., Tarantino, V., Vallesi, A., & Bisiacchi, P. (2015). Spatiotemporal neurodynamics underlying internally and externally driven temporal prediction: A high spatial resolution ERP study. *Journal of Cognitive Neuroscience*, 1–15.
Mento, G. (2013). The passive CNV: Carving out the contribution of task-related processes to expectancy. *Frontiers in Human Neuroscience, 7*, 827.
Monfort, V., Pouthas, V., & Ragot, R. (2000). Role of frontal cortex in memory for duration: An event-related potential study in humans. *Neuroscience Letters, 286*, 91–94.
Nagahama, Y., Okada, T., Katsumi, Y., Hayashi, T., Yamauchi, H., Oyanagi, C., et al. (2001). Dissociable mechanisms of attentional control within the human prefrontal cortex. *Cerebral Cortex, 11*, 85–92.
Nobre, A., Correa, A., & Coull, J. (2007). The hazards of time. *Current Opinion in Neurobiology, 17*(4), 465–470.
Norman, K. A., Polyn, S. M., Detre, G. J., & Haxby, J. V. (2006). Beyond mind-reading: Multi-voxel pattern analysis of fMRI data. *Trends in Cognitive Science, 10*, 424–430. https://doi.org/10.1016/j.tics.2006.07.005.
Oldfield, R. C. (1971). The assessment and analysis of handedness: The Edinburgh inventory. *Neuropsychologia, 104*, 199–206.
Perri, R. L., Berchicci, M., Lucci, G., Spinelli, D., & Di Russo, F. (2014a). The premotor role of the prefrontal cortex in response consistency. *Neuropsychology, 29*, 767. https://doi.org/10.1037/neu0000168.
Perri, R. L., Berchicci, M., Lucci, G., Spinelli, D., & Di Russo, F. (2014b). Individual differences in response speed and accuracy are associated to specific brain activities of two interacting systems. *Frontiers in Behavioral Neuroscience, 8*, 251.
Perri, R. L., Berchicci, M., Lucci, G., Spinelli, D., & Di Russo, F. (2015). Why do we make mistakes? Neurocognitive processes during the preparation-perception-action cycle and error-detection. *NeuroImage*. https://doi.org/10.1016/j.neuroimage.2015.03.040.
Perri, R. L., Berchicci, M., Lucci, G., Spinelli, D., & Di Russo, F. (2016). Fixing errors: How the brain prevents a second error in a decision-making task. *Scientific Reports, 6*, 32058. https://doi.org/10.1038/srep32058.
Pfeuty, M., Ragot, R., & Pouthas, V. (2005). Relationship between CNV and timing of an upcoming event. *Neuroscience Letters, 382*, 106–111.
Pfeuty, M., Ragot, R., & Pouthas, V. (2003). Processes involved in tempo perception: A CNV analysis. *Psychophysiology, 40*, 69–76.
Posner, M. I., Snyder, C. R., & Davidson, B. J. (1980). Attention and the detection of signals. *Journal of Experimental Psychology: General, 109*, 160–174.
Ragazzoni, A., Di Russo, F., Fabbri, S., Pesaresi, I., Di Rollo, A., Perri, R. L., et al. (2019). "Hit the missing stimulus". A simultaneous EEG-fMRI study to localize the generators of endogenous ERPs in an omitted target paradigm. *Scientific Reports, 9*(1), 3684.
Requin, J. (1969). Some data on neurophysiological processes involved in the preparatory motor activity to reaction time performance. *Acta Psychologica, 30*, 358–367.
Rosa, M. J., Daunizeau, J., & Friston, K. J. (2010). EEG-fMRI integration: A critical review of biophysical modeling and data analysis approaches. *Journal of Integrative Neuroscience, 9*, 453–476.
Ruchkin, D. S., Canoune, H. L., Johnson, R., & Ritter, W. (1995). Working memory and preparation elicit different patterns of slow wave event-related brain potentials. *Psychophysiology, 32*, 399–410.
Sakai, K., Hikosaka, O., Takino, R., Miyauchi, S., Nielsen, M., & Tamada, T. (2000). What and when: Parallel and convergent processing in motor control. *The Journal of Neuroscience, 20*(7), 2691–2700.
Shibasaki, H., & Hallett, M. (2006). What is Bereitschaftspotential? *Clinical Neurophysiology, 117*, 2341–2356.
Snyder, A. Z., Abdullaev, Y. G., Posner, M. I., & Raichle, M. E. (1995). Scalp electrical potentials reflect regional cerebral blood flow responses during processing of written words. *Proceedings of the National Academy of Sciences of the United States of America, 92*, 1689–1693.
Sulpizio, V., Committeri, G., & Galati, G. (2014). Distributed cognitive maps reflecting real distances between places and views in the human brain. *Frontiers in Human Neuroscience, 8*, 716.
Sulpizio, V., Lucci, G., Berchicci, M., Galati, G., Pitzalis, S., & Di Russo, F. (2017). Hemispheric asymmetries in the transition from action preparation to execution. *NeuroImage, 148*, 390–402.
Talairach, J., & Tournoux, P. (1988). *Co-planar stereotaxic atlas of the human brain.* New York: Thieme.
Trillenberg, P., Verleger, R., Wascher, E., Wauschkuhn, B., & Wessel, K. (2000). CNV and temporal uncertainty with "ageing" and "non-ageing" S1–S2 intervals. *Clinical Neurophysiology, 111*(7), 1216–1226.
Triviño, M., Correa, A., Arnedo, M., & Lupiáñez, J. (2010). Temporal orienting deficit after prefrontal damage. *Brain, 133*, 1173–1185.
Vallesi, A., McIntosh, A. R., Shallice, T., & Stuss, D. T. (2009). When time shapes behavior: fMRI evidence of brain correlates of temporal monitoring. *Journal of Cognitive Neuroscience, 21*(6), 1116–1126.
Vallesi, A., Mussoni, A., Mondani, M., Budai, R., Skrap, M., & Shallice, T. (2007). The neural basis of temporal preparation: Insights from brain tumor patients. *Neuropsychologia, 45*(12), 2755–2763.
van Boxtel, G. (1994). *Non-motor components of slow brain potentials.* Doctoral dissertationTilburg, Holland: Tilburg University.
van Boxtel, G. J., & Böcker, K. B. (2004). Cortical measures of anticipation. *Journal of Psychophysiology, 18*(2–3), 61–76.
Vaughan, H. G., Jr, Costa, L. D., & Ritter, W. (1968). Topography of the human motor potential. *Electroencephalography and Clinical Neurophysiology, 25*, 1–10.
Walter, W. G., Cooper, R., Aldridge, V. J., McCallum, W. C., & Winter, W. G. (1964). Contingent negative variation: An electrical sign of sensorimotor association and expectancy in the human brain. *Nature, 203*, 380–384.
Warm, J. S., Parasuraman, R., & Matthews, G. (2008). Vigilance requires hard mental work and is stressful. *Human Factors, 50*, 433–441.